Computational Complexity Reduction in Taguchi Method Based Joint Optimization of Antenna Parameters in LTE-A Networks

A Thesis presented in partial fulfilment of the

Requirements for the degree of

Master of Engineering

In

Telecommunication and Network Engineering

By

Yongfeng Diao

SCHOOL OF ENGINEERING AND ADVANCED TECHNOLOGY

MASSEY UNIVERSITY

PALMERSTON NORTH

NEW ZEALAND

JUNE 2013

ABSTRACT

Long Term Evolution-Advanced (LTE-A) system is operated with cellular technology based on frequency reuse. Due to the co-channel interference between cells, one cell's performance is decided by not only its own configurations but also other cell's settings. Therefore, joint optimization of antenna parameters in LTE-A cellular networks is the key to maximizing coverage and capacity. This can be achieved by setting the antenna parameters such as azimuth orientations and tilts to the optimal values. Nevertheless, the large number of cell parameters and the interdependencies between these parameters make it difficult and time-consuming to optimize a cellular network. In practice, the joint setting of the parameters of all cells with irregular layout and coverage areas becomes an important and challenging task.

There are several methods to search for the optimal settings of a cellular network. One commonly used search method is Simulated Annealing (SA). SA can produce good results in cellular network optimization, but it takes a long time and its performance can easily be degraded if the input parameters are misconfigured. Other methods include the trial-and-error approach that requires manual selection of parameter values and has no guarantee for good results, and the brute-force approach that searches through all possible combinations of parameter values and is thus computationally prohibitive.

Among the various algorithms proposed for this time-consuming optimization task, the iterative approach based on the Taguchi method (TM) is a recent development that has been shown to be promising. This thesis presents some further improvements to the TM-based approach aiming at enhancing optimization performance and reducing computational complexity. The proposed improvements include the use of the mixed-level Nearly-Orthogonal Array (NOA) to cater for the different optimization ranges of different types of parameters, an improved mapping function to select testing values that are more representative of the optimization range, and a hybrid approach using multiple NOAs with decreasing number of experiments to exchange small degradation in optimization performance for significant reduction in computational complexity. The effectiveness of the proposed improvements is demonstrated by numerical examples.

ACKNOWLEDGEMENTS

First I would like to thank my supervisor Dr. Xiang Gui for his excellent guidance and very helpful comments on my background studies.

I also thank Dr. Min Zhang and Mr. Aaron Dow from Alcatel-Lucent for their support and encouragement throughout the project.

Furthermore, I would like to thank Ministry of Science and Innovation (MSI) of New Zealand for the Education Fellowship that supported me to finish this project.

Finally, I am immensely indebted to my wife and my children for their love and support throughout my studies.

To my wife and my children

CONTENTS

Abbreviations

3G	Third Generation
3GPP	Third Generation Partnership Project
3GPP2	Third Generation Partnership Project 2
AM	Arithmetic Mean
ANR	Automatic Neighbor Relation
ARQ	Automatic Repeat-reQuest
ATM	Asynchronous Transfer Mode
AWGN	Additive White Gaussian Noise
BCH	Broadcast Channel
BLER	Block Error Ratio
BS	Base Station
CA	Carrier Aggregation
CCO	Coverage and Capacity Optimization
CDD	Cyclic Delay Diversity
CDF	Cumulative Distribution Function
CDMA2000	Code Division Multiple Access 2000
CIO	Cell Individual Offset
CQI	Channel Quality Indicator
CRC	Cyclic Redundancy Check
CRS	Cell-specific Reference Signals
CS	Circuit Switch
CSI	Channel State Information
CSI-RS	Channel State Information Reference Signals
DCI	Downlink Control Information
DECT	Digital Enhanced Cordless Telecommunications
DFT	Discrete Fourier Transform
DL-SCH	Downlink Shared Channel
DM-RS	Demodulation Reference Signals
DNS	Domain Name System
DynaTAC	Dynamic Adaptive Total Area Coverage
EDGE	Enhanced Data rates for Global System for Mobile Communications Evolution
eNodeB	Enhanced NodeB
EPC	Evolved Packet Core

ETSI	European Telecommunications Standards Institute
FDD	Frequency Division Duplex
FFT	Fast Fourier Transform
FLMTS	Future Land Mobile Telecommunication System
FMCA	Fixed Mobile Convergence Alliance
GA	Genetic Algorithm
GCI	Global Cell Identity
GPRS	General Packet Radio Service
GSM	Global System for Mobile Communications
HM	Harmonic Mean
HNB	Home Node B
HO	Hand Over
HSPA	High Speed Packet Access
HSS	Home Subscriber Server
ICIC	Inter-Cell Interference Coordination
IEEE	Institute of Electrical and Electronics Engineers
IETF	Internet Engineering Task Force
IFFT	Inverse Fast Fourier Transform
IMT	International Mobile Telecommunications
IMT-Advanced	International Mobile Telecommunications Advanced
IMS	IP Multimedia Subsystem
IP	Internet Protocol
IR	Incremental Redundancy
IRC	Interference Rejection Combination
ISP	Internet Service Provider
ITU	International Telecommunications Union
LD	Level Difference
LTE/LTE-A	Long Term Evolution/ Long Term Evolution Advanced
MAC	Medium Access Control
MBSFN	Multicast Broadcast Single Frequency Network
MCH	Multicast Channel
MIMO	Multiple-Input and Multiple-Output
MME	Mobility Management Entity
MRC	Maximum Ratio Combination
MRO	Mobility Robustness Optimization
MU-MIMO	Multi-User MIMO

NGMN	Next Generation Mobile Networks
NLoS	Non Line of Sight
NMT	Nordic Mobile Telephone
NOA	Nearly-Orthogonal Array
OA	Orthogonal Array
OFDM	Orthogonal Frequency-Division Multiplexing
OFDMA	Orthogonal Frequency-Division Multiple Access
OMA	Open Mobile Alliance
OPEX	Operational Expenditure
OSS	Operation Support System
PCFICH	Physical Control Format Indicator Channel
PCH	Paging Channel
PCI	Physical Cell ID
PDC	Personal Digital Cellular
PDCCH	Physical Downlink Control Channel
PDCP	Packet Data Convergence Protocol
PDN-G	Packet Data Network Gateway
PHICH	Physical Hybrid-ARQ Indicator Channel
PMI	Pre-coder Matrix Indication
POT	PCI Optimization Tool
PPT	PCI Planning Tool
PRBs	Physical Resource Blocks
PUCCH	Physical Uplink Control Channel
PUSCH	Physical Uplink Shared Channel
QAM	Quadrature Amplitude Modulation
QoE	Quality of Experience
QoS	Quality of Service
QPP	Quadrature Permutation Polynomial
QPSK	Quadrature Phase-Shift Keying
RACH	Random Access Channel
RAN	Radio Access Network
RAT	Radio Access Technology
RF	Radio Frequency
RFC	Request For Comments
RI	Rank Indication
RLC	Radio Link Control

RLF	Radio Link Failures
RM	Rate Matching
RNC	Radio Network Controller
RRC	Radio Resource Control
R-PDCCH	Relay Physical Downlink Control Channel
SA	Simulated Annealing
SAE	System Architecture Evolution
SDMA	Space Division Multiple Access
Serving-GW	Serving Gateway
SGSN	Serving General Packet Radio Services Support Node
SIC	Successive Interference Cancellation
SIP	Session Initiation Protocol
SNR	Signal to Noise Ratio
SINR	Signal to Interference and Noise Ratio
SON	Self- Organizing Network
SRS	Sounding Reference Signals
STBD	Space Time Block Coding
STTD	Space Time Transmit Diversity
TA	Traffic Area
TAI	TA Identifier
TAP	Tracking Area Planning
TAU	TA Updates
TM	Taguchi Method
TX	Transmitter
TDD	Time Division Duplex
TDMA	Time Division Multiple Access
TD-SCDMA	Time Division-Synchronous Code Division Multiple Access
TTI	Transmission Time Interval
TTT	Time-To-Trigger
UE	User Equipment
UL-SCH	Uplink Shared Channel
UMa	Urban Macro
UMTS	Universal Mobile Telecommunication System
VHE	Virtual Home Environment
VLAN	Virtual Local Area Network
WCDMA	Wideband Code Division Multiple Access

WiMAX	Worldwide interoperability for Microwave Access
WLAN	Wireless Local Area Network

List of Figures

List of Tables

1 Introduction

Succeeding 3G networks, Long Term Evolution (LTE) has been developed as a new mobile communication standard for the next generation. The LTE is often called “4G”, and 4G networks have more features and advantages than 3G networks. In 4G networks, there are better coverage and faster data rate than 3G networks. LTE is the true 4G evolution step and shares the same technology with LTE-Advanced (LTE-A). As a further enhancement to LTE, LTE-A is a continuing task within the Third Generation Partnership Project (3GPP).

The target of LTE-A mobile technologies is for use in all computers and mobile Internet access devices. Its coverage will be used for customers to have wireless broadband access, which does not need any cabling. Users can enjoy a worldwide mobile service and a high speed downlink and uplink service under 4G networks [1].

The core network of LTE-A is based on Orthogonal Frequency-Division Multiple Access (OFDMA) by using Multiple-Input and Multiple-Output (MIMO) and Self-Organizing Network (SON) technologies. The MIMO technology increases transmit speed in LTE-A networks. The SON technology has many Artificial Intelligence (AI) functions including automatic software download, automatic inventory, automatic Physical Cell ID (PCI) assignment, mobility optimization, Inter-Cell Interference Coordination (ICIC), coverage optimization, and energy saving.

In LTE-A, optimizing antenna azimuth orientations and tilts can increase cellular network Base Station (BS) coverage and capacity to improve User Equipment (UE) performance. This can be achieved by setting the antenna parameters such as azimuth orientations and tilts to the optimal values. Due to the interdependencies between these parameters, finding the optimal configuration is a time-consuming and complex task. Among the various algorithms proposed for this task, the joint optimization approach based on the Taguchi method (TM) is a recent development that has been shown to be promising. In this thesis, we will present an improved TM to find near-optimal values for radio network parameters in the LTE-A network. The proposed improvements include the use of the mixed-level Nearly-Orthogonal Array (NOA) to cater for the different optimization ranges of different types of parameters, an improved mapping function to select testing values that are more representative of the optimization range,

and a hybrid approach using multiple NOAs with decreasing number of experiments to exchange small degradation in optimization performance. The improved TM uses less computation to achieve better results than existing TM in the joint optimization search.

1.1 Scope and Goals of the Thesis

This thesis is focused on the optimization of antenna parameters to improve the downlink performance of LTE-A networks using system level simulation, with reduced computational complexity. The research work has three parts as follows:

a. Comparison of mixed-level NOA employing existing or improved mapping function and the identical-level NOA in TM-based optimization
b. Comparison of the hybrid approach using multiple mixed-level NOAs employing existing mapping function and the identical-level NOA in TM-based optimization
c. Comparison of single mixed-level NOA employing improved mapping function, the hybrid approach using multiple mixed-level NOAs employing improved mapping function with different iteration schemes, and the identical-level NOA in TM-based optimization

1.2 Structure of the Thesis

The thesis starts with LTE-A introduction by describing the LTE-A network architecture, high data rates and some technical features in Chapter 2. Chapter 3 covers SON in LTE-A network, describing SON in Next Generation Mobile Networks (NGMN) and some SON features in the cellular network. Chapter 4 gives an overview of various optimization algorithms employed in cellular network optimization. Chapter 5 details the optimization problem in LTE-A network, the procedure of TM-based joint optimization together with the proposed use of mixed-level NOA, improved mapping function, and multiple mixed-level NOAs. An analysis on the optimization range shrinkage considering the effect of multiple NOAs is also presented in Chapter 5, along with details of the LTE-A system model used in testing the TM-based optimization algorithm with the proposed improvements. Chapter 6 presents simulation algorithm parameters and simulation results. Chapter 7 summarizes the research work and provides suggestion on further research.

2 Long Term Evolution Advanced (LTE-A)

In 2002, the International Telecommunication Union (ITU) designated International Mobile Telecommunications Advanced (IMT-Advanced) to 4G mobile networks. The goal is that the majority of users will be able to connect to a wireless network at any point in the world. In 2005, the third Generation Partnership Project (3GPP) started work on the LTE standard, the trademarked project name for a step toward the 4G. There are two major competing standards in 4G mobile technology. One standard is Worldwide interoperability for Microwave Access (WiMAX), and the other is LTE. Both WiMAX and LTE are based on OFDMA and MIMO technologies, and they are using Internet Protocol (IP) networks with Quality of Service (QoS).

2.1 Standardization

Setting a standard for mobile communication normally includes four parts: requirements, architecture, detailed specifications, and testing and verification. LTE is a 3GPP standard that is based on OFDMA and smart antennas. The 3GPP Release 9 was published in December 2009. It includes LTE home NodeB, location services, Multimedia Broadcast/Multicast Service (MBMS), and Multi-standard BS. The recent release was Release 11 in March 2012. It is named LTE-Advanced and includes carrier aggregation, enhanced downlink MIMO, uplink MIMO, enhanced ICIC and relays. The LTE main features include low delay and high data rate at the cell edge, spectrum flexibility, capacity and peak data rate requirements, and maximum commonality between Time Division Duplex (TDD) and Frequency Division Duplex (FDD) solutions.

The LTE-A is not a new technology. It is an evolution of LTE from further developments of the 3GPP network. The features of LTE-A are part of Release 10 of 3GPP LTE specifications. The IMT-advanced target needs LTE-A to reach wider bandwidth through aggregation of multiple carriers, and uses advanced antenna techniques in uplink and downlink. Table 2-1 shows the LTE-A evolution from the 3G services [2].

Table 2-1: LTE-Advanced evolution

	WCDMA (UMTS)	HSPA HSDPA/HSUPA	HSPA+	LTE	LTE Advanced (IMT Advanced)
Max downlink speed bps	384k	14M	28M	100M	1G
Max uplink speed bps	128k	5.7M	11M	50M	500M
Latency round trip time approx.	150ms	100ms	50ms (max)	~10ms	Less than 5ms
3GPP release	Rel. 99/4	Rel.5/6	Rel.7	Rel.8	Rel.10
Approx. years of initial roll out	2003/4	2005/6 HSDPA 2007/8 HSUPA	2008/9	2009/10	2010
Access methodology	CDMA	CDMA	CDMA	OFDMA/SC-FDMA	OFDMA/SC-FDMA

The early release of LTE already supported for deployment in spectrum allocations having different characteristics. In Release 10, the Carrier Aggregation (CA) can further extend transmission bandwidth. There are up to five component carriers that can be jointly used for transmission in different bandwidth, and can be aggregated allowing for transmission bandwidths up to 100MHz. The extended multi-antenna in Release 10 is expanded to support up to eight transmission layers in downlink spatial multiplexing. This enables downlink data rates up to 3 Gbits/s or 30 bit/s/Hz. The uplink spatial multiplexing is extended up to four layers and this technology can be used for uplink transmit-side beam-forming. The uplink carrier aggregation allows uplink data rates up

to 1.5 Gbit/s or 15 bit/s/Hz. The relay is the LTE-based wireless backhaul; it is providing an easy way to improve coverage. The relay node is a low power base station like an ordinary cell.

The User Equipment (UE) category has many different parameters in different LTE release [3, Page 106]. Table 2-2 shows clearly details of different release category parameters.

Table 2-2: Releases of LTE

	Category							
	Release 8/9/10				Release 10 only			
	1	2	3	4	5	6	7	8
Downlink peak rate (Mbit/s)	10	50	100	150	300	300	300	3000
Uplink peak rate (Mbit/s)	5	25	50	50	75	50	150	1500
Maximum downlink modulation	64QAM							
Maximum uplink modulation	16QAM			64QAM	16QAM		64QAM	
Maximum number of layers for downlink spatial multiplexing	1	2			4	Signaled separately		

2.2 Network Architecture

The LTE BS is different from UMTS BS. The LTE BS is called Enhanced NodeB (eNodeB). There is no central controlling element in the radio network: the eNodeB manages air interface traffic and QoS. The eNodeB can also communicate with each other the handovers for active mobiles via X2 interface [4, Page 47]. The interface that connects the eNodeB to the core network and the radio network is the S1 interface. The S1 interface is based on the IP protocol and transport technology. In contrast, the UMTS interface between the NodeB, the Radio Network Controller (RNC) and the Serving General Packet Radio Services (GPRS) Support Node (SGSN) are based on the Asynchronous Transfer Mode (ATM) protocol. The ATM only provides 2 Mbit/s connections. LTE BSs are equipped with 1 Gbit/s Ethernet fibre ports.

As can be seen in Figure 2-1, there are two logical entities, the Serving Gateway (Serving-GW) and Mobility Management Entity (MME), splitting the radio access network from the core network. The MME is the ‘control plane’. Its functions include authentication, handover support for each eNodeB to different radio networks, establishment of radio bearers between subscriber mobility and session management signalling. The MME also can trace mobile devices in idle mode and selection of a gateway to Internet from the network. The Serving Gateway is focused on the customer part. It is utilized for forwarding IP packets between the Internet and mobile devices. The S1 interface connects user data to the Serving- GW and signalling data to the MME. Thus, the S1 interface is split into two protocols: the S1-C (Control) interface and the S1-U (User) interface. The S1-C is used to control messages between the MME and a mobile device, and the messages use non-IP channels over the air interface. The S1-U is like IP packets over the air interface to the Serving-GW. Between the MME and the Serving GW, the S11 interface is used to connect them [4, Page 47].

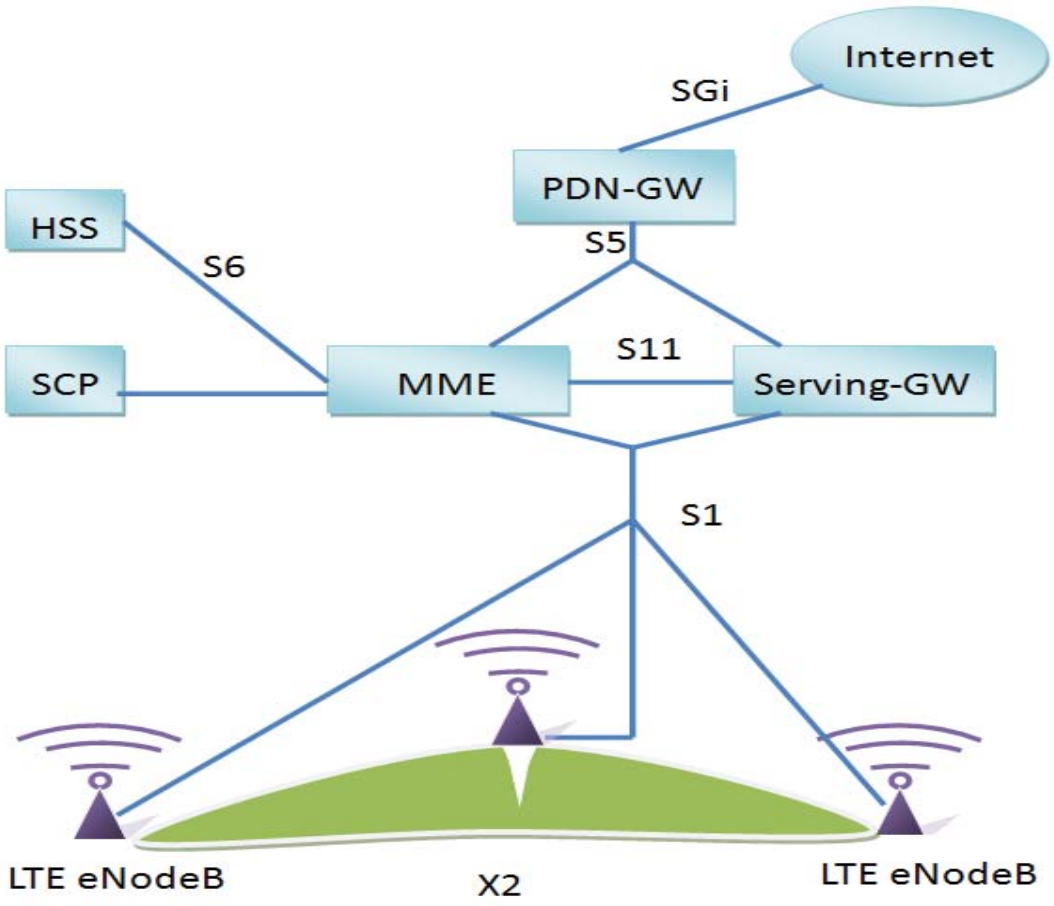

Figure 2-1: LTE network architecture

In LTE, the router can be likened to the Packet Data Network Gateway (PDN-GW) in the network. The number of users decides the number of PDN-GWs and the capabilities of the hardware. As Figure 2-1 shows, the S5 interface connects between the PDN-GW and the MME/Serving-GW in LTE. The S5 is managed by different Serving-GW for the establishment of a user data tunnel and subsequent tunnel modifications when the user moves from one cell to other cells. The Home Subscriber Server (HSS) and Service Control Point (SCP) connect with MME via the S6 interface. The HSS is the database that stores subscription information for UMTS, GPRS, GSM, LTE and IP Multimedia Subsystem (IMS).

The big difference of LTE from UMTS and GSM is that LTE always uses an IP address in the network. As Figure 2-2 shows, when a user moves from the LTE coverage area to a UMTS network, the mobile device reports to the eNodeB that a UMTS (or GSM) cell has been found. The hand over procedure starts from the MME that receives the report and communicates with LTE eNodeB. The S3 interface is based on IP protocol used for

SGSN relocation procedures. There is no need to change the interface to 3G SGSN to communication between LTE and 3G network. When 3G network is ready for the handover, the MME sends a handover signal to eNodeB to execute handover. After the handover, the MME is released, and the subscriber management and 3G SGSN takes over this work. The user data is delivered via the S4 interface from Serving-GW to 3G SGSN [4, Page 50].

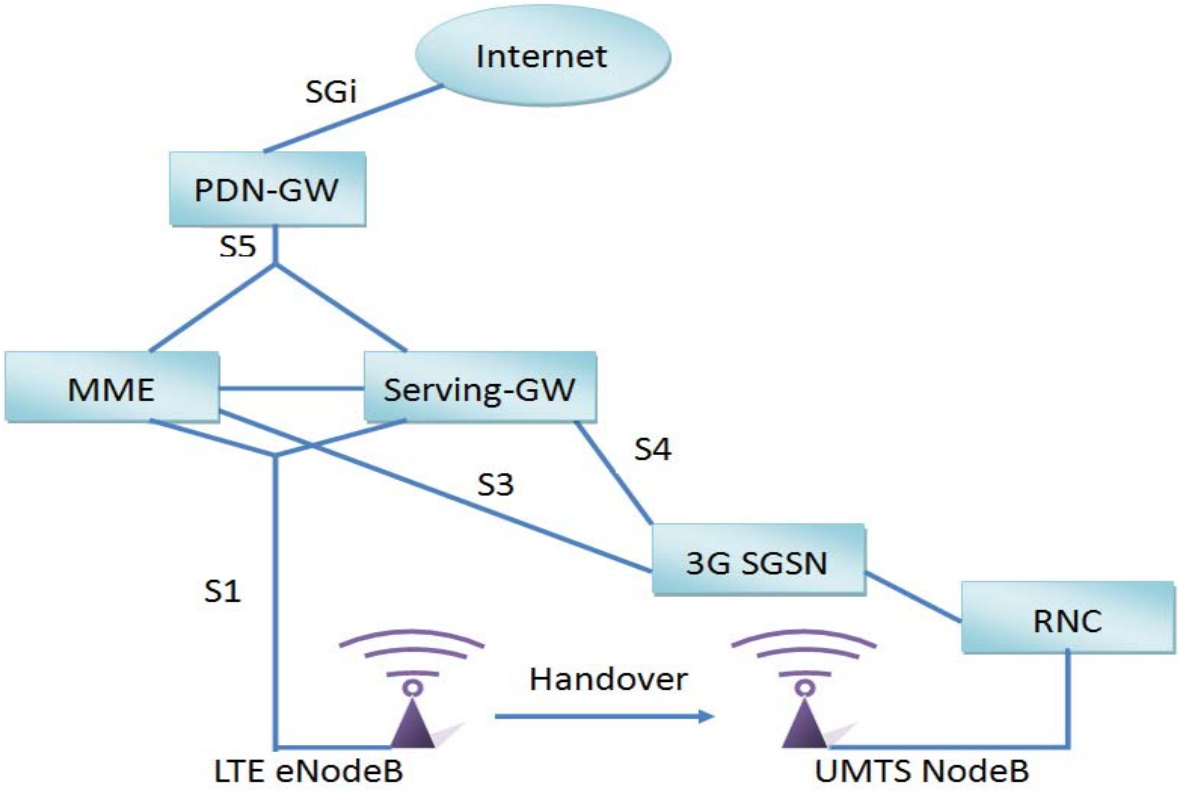

Figure 2-2: LTE and 3G network architecture

2.3 Multiple Antennas

2.3.1 Benefits of Multi-Antenna

Multi-antenna techniques improve system performance, system capacity, coverage of cell and service provisioning. The distance between the different antenna elements is an important characteristic of multi-antenna. Multiple antennas need a large inter-antenna distance or different antenna polarizations to work against fading over the radio channel. Beam-forming can be used in multiple antennas at the transmitter or receiver to against high or low fading correlation between the antennas. Multiple parallel communication channels can be created by the simultaneous use of multiple antennas at the transmitter

over the radio interface. It enables high data rates within a narrow bandwidth. It is known as MIMO when multiple antennas are employed at both the transmitter and the receiver.

2.3.2 Multiple Receive Antennas

Multiple receive antennas are often used for receive diversity to combat radio channel fading. Maximum Ratio Combination (MRC) is an antenna combining goal when the received signal is impaired by noise. The MRC principles are to phase rotate the signals received at the multiple antennas to ensure that the signals are phase aligned by compensating for the corresponding channel phases; and to apply higher weights in proportion to their corresponding channel gains.

In many cases of mobile communication the interference from other transmitters within the system is stronger than noise. When some numbers of interfering signals have equal strength from the base station, the interferer is suppressed after the MRC. An interfering terminal may be in the same cell as the target terminal or in a neighbouring cell. A better way to select the antenna weight is referred to as Interference Rejection Combination (IRC) [3, Page 62].

2.3.3 Multiple Transmit Antennas

Multiple antennas can provide diversity and beam-forming at the transmitter side. At the terminal, there is no need for additional receive antennas and corresponding receiver chains. In a radio link with multi-path propagation, the transmitted signal is sent to the receiver through multiple, independently fading paths with many different delays. The transmission scheme has tools to counteract signal corruption, because of the radio-channel frequency selectivity. Multiple transmit antennas can create artificial time dispersion or artificial frequency selectivity for some channels that are not time dispersive. The delay diversity needs to ensure suitable frequency selectivity over the bandwidth of the signal. Cyclic Delay Diversity (CDD) is like the normal delay diversity, but the CDD operates block wise and applies cyclic shifts that like a linear delay [3, Page 67]. Space Time Transmit Diversity (STTD) is a scheme of Space Time Block Coding (STBC) using two antennas. It is also a part of the 3G WCDMA standard in the first release. Figure 2-3 shows STTD runs on a couple of modulation symbols.

The first antenna transmits the modulation symbols. The second antenna transmits reversed modulation symbols. So the STTD transmission can be expressed as: $\bar{r} = \begin{pmatrix} r_{2n} \\ r_{2n+1} \end{pmatrix} = \begin{pmatrix} h_1 & -h_2 \\ h_2 & h_1 \end{pmatrix} \cdot \begin{pmatrix} s_{2n} \\ s_{2n+1} \end{pmatrix} = H \cdot \bar{s}$. The output symbol rate of the two antenna space time coding of Figure 2-3 is the same as the input symbol rate [3, Page 67].

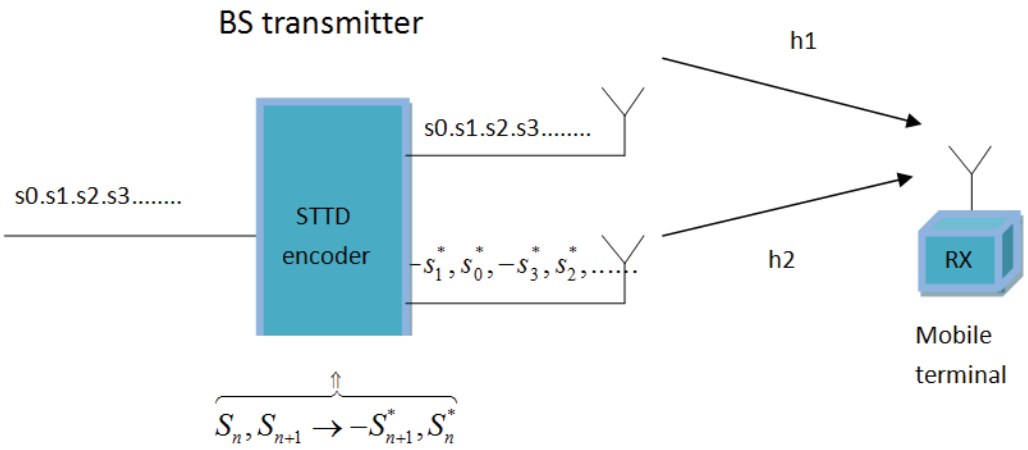

Figure 2-3: Space-Time Transmit Diversity (STTD)

In LTE, multi-antenna transmission is a mapping from the output of the data modulation to different antennas ports. Each of the Transmission Time Interval (TTI) in every transport block is used to benefit more from the effect of interleaving and to increase the efficiency of error-correction. Different transmission modes have different multi-antenna transmission schemes. Table 2-3 summarizes the currently defined transmission modes and their transmission schemes.

Table 2-3: Transmission modes and schemes

Transmission mode 1:	Single-antenna transmission.
Transmission mode 2:	Transmit diversity.
Transmission mode 3:	Open-loop codebook-based pre-coding in the case of more than one layer, transmit diversity in the case of rank-one transmission.

Transmission mode 4:	Closed-loop codebook-based pre-coding.
Transmission mode 5:	Multi-user-MIMO version of transmission mode 4.
Transmission mode 6:	Special case of closed-loop codebook-based pre-coding limited to single layer transmission.
Transmission mode 7:	Release-8 non-codebook-based pre-coding supporting only single layer transmission.
Transmission mode 8:	Release-9 non-codebook-based pre-coding supporting up to two layers.
Transmission mode 9:	Release-10 non-codebook-based pre-coding supporting up to eight layers.

2.3.4 Spatial Multiplexing

For higher data rates and more efficient utilization of spectrum, multiple antennas can be employed at both the transmitter and the receiver for spatial multiplexing. For Additive White Gaussian Noise (AWGN) channel, the channel capacity is $C = BW \cdot \log_2\left(1 + \frac{S}{N}\right)$ or $\frac{C}{BW} = \log_2\left(1 + \frac{S}{N}\right)$, where C is the channel capacity, BW is the bandwidth available for the communication, S is the received signal power, and N is the power of the white noise impairing the received signal. With spatial multiplexing, the channel capacity is $\frac{C}{BW} = N_L \cdot \log_2\left(1 + \frac{N_R}{N_L} \cdot \frac{S}{N}\right) = \min\{N_T, N_R\} \cdot \log_2\left(1 + \frac{N_R}{\min\{N_T, N_R\}} \cdot \frac{S}{N}\right)$, where N_T is the number of transmit antennas and N_R is the number of receive antennas, and $N_L = \min\{N_L, N_R\}$[3, Page 73]. Figure 2-4 shows a 2X2 configuration with two transmit antennas and two receiver antennas. Assuming that there is no radio channel time dispersion, the received signals can be expressed as: $\bar{r} = \begin{pmatrix} r_1 \\ r_2 \end{pmatrix} = \begin{pmatrix} h_{1.1} & h_{1.2} \\ h_{2.1} & h_{2.2} \end{pmatrix} \cdot \begin{pmatrix} s_1 \\ s_2 \end{pmatrix} + \begin{pmatrix} n_1 \\ n_2 \end{pmatrix} = H \cdot \bar{s} + \bar{n}$ [3, Page 67].

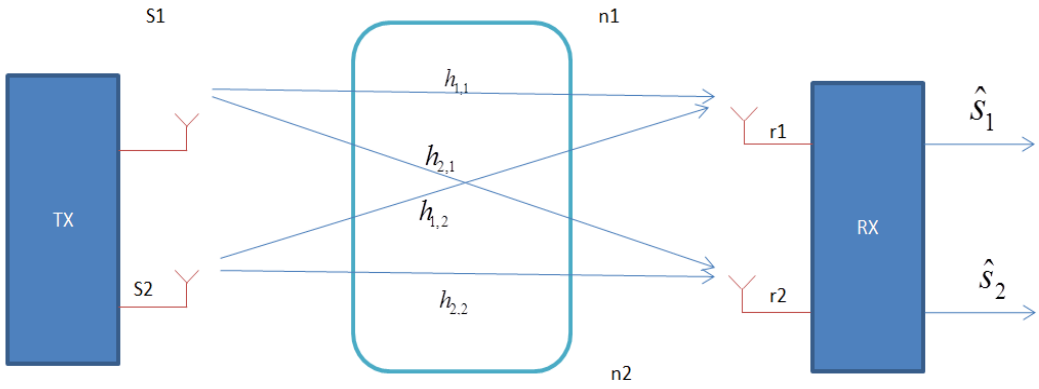

Figure 2-4: 2X2 antenna configuration

On the receive side, the nonlinear approach of Successive Interference Cancellation (SIC) is used in the demodulation of spatially multiplexed signals.. In SIC, the first spatially multiplexed signal is demodulated and decoded in the receiver. If the decoded data is correct, the second signal is then demodulated and decoded, and the process continues until all spatially multiplexed signals have been demodulated and decoded.

Spatial multiplexing is multiple parallel transmissions using the same time-frequency resource to the same terminal. It is also known as MIMO transmission. The Multi-User MIMO (MU-MIMO) communicates to different terminals in the same time-frequency resource, and it relies on multiple antennas at transmitter side. In MU-MIMO transmission, all terminals would need to have exactly the same resource assignment, and also the full set of receive antennas. There are two types of MU-MIMO in 3GPP network, one is part of transmission modes 8 and 9 based on non-codebook-based pre-coding, and the transmission modes 3, 4, 5 and 6 are based on codebook-based pre-coding.

2.4 Radio Frequency

2.4.1 Radio Frequency Characteristics

Radio waves are a type of electromagnetic radiation. The International Telecommunication Union (ITU) defines that the range of radio frequency spectrum is from 3 kHz to 3000 GHz. The Radio frequency spectrum is a limited natural resource. People need to utilize the resource more efficiently and safely. In the world, different

countries use different allocations of radio frequencies. Most countries have radio spectrum management group managing the radio spectrum policy, planning, license registration, interference and compliance. ITU divides the world into three regions, with each region having its own frequency allocations. The first region is Europe and Africa, the second is America, and the third region is Asia and Australasia. Table 2-4 shows the radio bands defined by ITU [5].

Table 2-4: ITU radio bands

Radio frequencies		
Abbreviation	Band	Range
VLF	Very Low Frequency	3 - 30 kHz
LF	Low Frequency	30 – 300 kHz
MF	Medium Frequency	300 kHz- 3 MHz
HF	High Frequency	3 – 30 MHz
VHF	Very High Frequency	30 – 300 MHz
UHF	Ultra High Frequency	300 MHz – 3 GHz
SHF	Super High Frequency	3 – 30 GHz
EHF	Extremely High Frequency	30 GHz – 300 GHz
THF	Tremendously high frequency	300- 3000 GHz

2.4.2 Radio Frequency for LTE

The RF BS transmits and receives RF signals on one or more antenna connectors in a physical node. The radio system requirement defined is fundamental for LTE. Due to LTE requires the multiple channel bandwidths and flexible bandwidth arrangement, the frequency bands of LTE include both paired and unpaired spectra. That means both FDD and TDD can be supported by LTE.

New bands are added continuously for every new release independent. IMT-2000 and IMT-Advanced chooses additional frequency bands for LTE. The following table lists the new frequency bands for LTE [6].

Table 2-5: IMT spectrum allocation

Frequency Bands	Regions
450-470 MHz	20 MHz wide for mobile service globally.
698-862 MHz	In Region 2 and nine countries of Region 3.
790-862 MHz	In Regions 1 and 3.
2300-2400 MHz	IMT identified for all three regions in the worldwide.
3400-3600 MHz	For some mobile service in Europe, Asia and some countries in the Americas.

3 Self-Organizing Network (SON) in LTE/LTE-A

The mobile wireless network is growing fast. If many network elements and associated parameters are manually configured, it will take a lot of time and increase operational costs. Even the manual process is potentially error-prone. SON helps improve network performance for higher user Quality of Experience (QoE), reduce operation error and operational expenses. Self-optimizing and self-organizing capabilities for LTE provide network intelligence, automation, optimization of wireless networks and network management features. Release 10 SON is proved that the SON has more benefits on network management than manual process. SON functions can be classified into two categories. The first category is for processes where automation can save time, reduce effort, and reduce deployment delay as compared to manual operation. The second is for processes that are too fast and too complex for manual intervention. SON will provide high quality and performance in LTE/LTE-A.

3.1 SON in Next Generation Mobile Network (NGMN)

SON concept has been included ever since the first release of LTE technology. It is a key component of the LTE network. The standardized SON features include: automatic inventory, automatic software download, automatic Physical Cell ID (PCI) assignment, mobility optimization, Inter-Cell Interference Coordination (ICIC), coverage and capacity optimization, energy savings, and more. The Next Generation Mobile Networks (NGMN) Alliance identifies the key use cases that are most important for carriers' day to day operations, providing guidance to the new technical standards being developed for LTE. Table 3-1 lists the top 10 use cases indicated by NGMN for LTE standards [7, Page 9].

Table 3-1: Top 10 NGMN use cases

1	**Plug and Play Installation**
2	Automatic Neighbor Relation configuration
3	OSS Integration

4	Handover Optimization
5	Minimization of Drive Tests
6	Cell Outage Compensation
7	Load Balancing
8	Energy Savings
9	Interaction macro/home BTS
10	QoS Optimization

The Operations Support System (OSS) is also an element of SON in NGMN, which includes support for open Operations Administration and Maintenance (OAM) interfaces and operator databases and tools. OSS in the SON should be able to indicate the configuration for BSs, and support neighbour cell detection and Auto Neighbour Relation (ANR) optimization.

3.2 Base Station (BS) Self-Configuration

New network technology provides more services, but its deployment is a major investment for the service provider. Costs on network planning, commissioning and integration are often higher than the infrastructure equipment itself. Traditionally, the installation of a new BS involves a lot of on-site configuration tasks and requires more than one expert engineer. The purpose of self-configuration SON is to reduce human intervention in the installation process by providing “plug and play” functionality in the BS.

Self-configuration involves many specific SON features including self-test, automatic software management, and automatic neighbour relation configuration. The self-configuration of BSs will result in a faster network deployment, reduced cost for the operator, and fewer errors. Figure 3-1 shows the different entities that are involved in the BS self-configuration in LTE [7, Page 14].

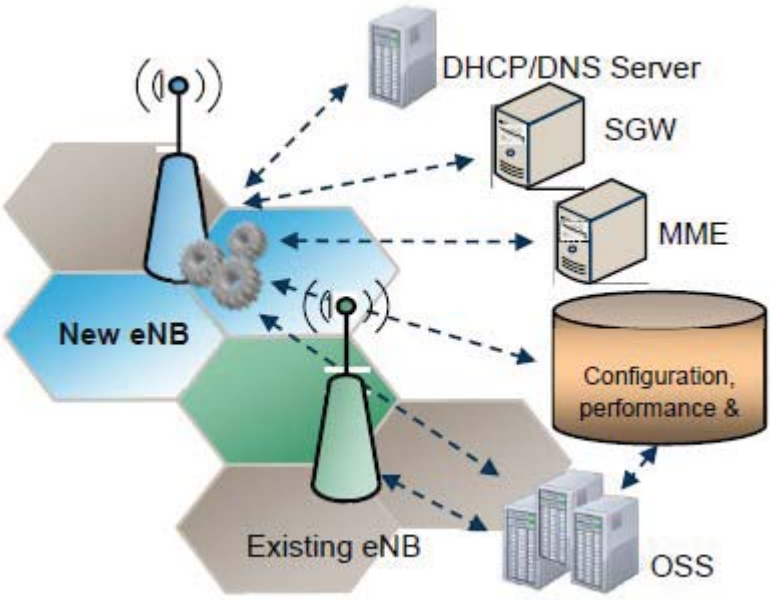

Figure 3-1: Self-configuration of eNB in LTE

A new eNodeB in a network should have access to the configuration server for a set of pre-configured RF parameters, including antenna configuration (type, height and azimuth), location, transmit power, initial neighbour configuration, cell identities and maximum configured capacity, as well as pre-planned transport parameters including Virtual Local Area Network (VLAN) partition, bandwidth and IP addresses. Also, the OSS should provide software update packages.

When a new eNB first boots, the self-configuration will begin with a self-test, followed by a set of self-detection functions. Then the eNB will connect to the DHCP/DNS servers requesting an IP address for itself and retrieving information about relevant servers such as the configuration server, SGW, and MME. This allows the eNB to acquire configuration parameters and update its eNB software. The self-optimization functions for finer parameter optimization are performed after the eNB is in operation state. In LTE standards, the self-configuration of eNB covers self-test, automatic software management, automatic inventory management, and automatic neighbour relation.

3.3 Inter-Cell Interference Coordination (ICIC)

Inter-Cell Interference Coordination (ICIC) is to be coordinated on the basis of the Physical Resource Blocks (PRBs) as LTE system is based on OFDMA and SC-FDMA. ICIC includes the following: users can be scheduled in units of a PRB which is 180 KHZ; neighbouring cells can coordinate which portions of the bandwidth are used in each cell and the transmission powers across various frequency resource blocks; and inter-cell interference can be reduced or avoided in uplink and downlink in the related cells by a coordinated usage of the available PRBs. ICIC leads to improved SINR, especially for cell edge UEs to achieve better edge rates and cell throughputs, and improved hand-off performance for cell edge UEs.

The goal of SON based ICIC is to eliminate interference and optimize the network automatically, with minimum human intervention in network management and optimization tasks. A SON ICIC includes the core ICIC algorithms, frequency planning and inter-eNB communications. The core ICIC algorithms determine how to manage the time, frequency and power resources to realize interference coordination between the cells. The performance of ICIC depends upon cell size, user mobility, cell load, traffic model, propagation channel, traffic type, etc.

3.4 Coverage and Capacity Optimization

Coverage and Capacity Optimization (CCO) is a typical task in wireless networks. It is achieved by adjusting the RF parameters of deployed cells. CCO is considered a key function of the self-optimization for SON. Self-optimizing coverage and capacity aims to provide optimal coverage and reduce manual operational tasks, resulting in Operational Expenditure (OPEX) reduction and user QoE improvement.

The self-optimizing CCO function is a continuous process that gathers measurements and takes corrective actions whenever necessary. CCO corrective actions include changes to antenna tilt and UL power control parameters. 3GPP specifications require that CCO should be performed with minimal human intervention; operator can control the objectives and targets for the CCO functions; operator can configure CCO in different areas of the network; and the collection of data used for CCO should be automated to the maximum extent possible with minimum dedicated resources.

4 Overview of Different Network Optimization Algorithms

4.1 Trial and Error

Trial-and-error is a heuristic method. It has other names such as “generate and test” and “guess and check”. Trial-and-error is a manual method in a network planning environment. In a small or simple network planning environment, the network performance can be improved quickly using this method. There is no rule in this method, but this does not mean that the approach is easy and suitable for all networks. Engineers using this method to optimize networks should have some knowledge in the area, and the approach is not suitable for large or complicated networks [8].

4.2 Brute-force Search

Brute-force search is an exhaustive search. It can find an optimal solution by searching through all candidate solutions, but the problem of brute-force search is that the number of candidate solutions is typically prohibitively large. For instance, if we test seven different antennas with 10 different values of azimuth orientation, the total number of candidate solutions to search is 10^7. If we increase the azimuth orientation range from 10 different values to 100, the size of the candidate solutions will be an unwelcome number. Brute-force search is only possible for problems with limited size. It can also be used as “baseline” method for benchmarking algorithms [9].

4.3 Tabu Search

Tabu search is a local search method for solving joint optimization problems. Tabu search uses intensification and diversification strategies in solving optimization problems. The intensification strategies use short-term memory function to search for a better solution based on the existing good solutions. It is focused on finding a best solution within a restricted region. The diversification strategies utilize long-term memory function to search a large region. Only the long-term is good for aggressively searching to get the best solution, but the disadvantage of diversification strategies is that if a search space includes large elements, it can fall into a small area of the search space. It is easy to miss the optimal value in a search space [10].

4.4 Genetic Algorithm

Genetic Algorithm (GA) was introduced by John Holland in the 1970s at University of Michigan. GA is a heuristic algorithm that mimics the natural selection process. It has been successfully applied to a wide variety of optimization problems in many fields. There are three major advantages with GA. Firstly, the GA works regardless the specific inner workings of the problem; secondly, GA is effective in a global search; thirdly, GA can incorporate problem-specific heuristics for efficient implementation. The disadvantages of GA are that there is no guarantee for finding the global optimal solution and the quality of the solution is highly dependent on the heuristic selection of initial values [11].

4.5 Simulated Annealing

Simulated Annealing (SA) is another heuristic local search algorithm. This method is proposed by Scott Kirkpatrick, C. Daniel Gelatt and Mario P. Vecchi in 1983 and by Vlado Cerny in 1985. SA can work in a large search space and could be more efficient than exhaustive enumeration [12]. As a heuristic algorithm, SA has the same disadvantages as GA [13].

4.6 Taguchi Method

Taguchi Method (TM) is designed for reducing the variation in a process through design of experiments. It was developed by Dr. Genichi Taguchi to produce high quality product at low cost to the manufacturer. The Taguchi's rule for manufacturing process has three stages. They are system design, parameter design and tolerance design [14]. The system design is a stage at the conceptual level. It is about process objective, or more specifically, a target value for the process performance. After the system design is completed, the design of experiments needs to create Orthogonal Arrays (OA) for the parameter design [15]. OA is an array that has a fixed finite set of integer members. Each member in OA appears the same number of times in every row and columns. OA generalize the idea of mutually orthogonal latin squares in a tabular form [16]. The last stage is Tolerance design. It is to control variation and reducing experiments in the critical few dimensions. Taguchi method is disputable in some of its statistical aspects, but this method is being successfully used in many areas, such as hardware design [17],

power electronics [18-20], microwave circuits [21] and optimization of communication and information networks [13].

5 Optimization Procedure Based on Taguchi's Method Using Multiple Mixed-Level NOAs

5.1 Introduction

Orthogonal Frequency-Division Multiple Access (OFDMA) provides high data rate services in Long Term Evolution/ Long Term Evolution Advanced (LTE/LTE-A) systems. Moreover, LTE-A system is operated with a frequency reuse factor of one. Thus optimizing cell coverage and capacity has become a very important task in LTE-A. In particular, radio network parameters such as antenna tilt and antenna azimuth orientation have strong impact on the network performance. Adjusting antenna tilts and antenna azimuth orientations affects the coverage and capacity drastically. Furthermore, due to the interactions among these parameters, tuning each of the parameters independently may not provide near-optimal solutions. An efficient way to increase network capacity and coverage is to optimize the radio network parameters jointly. While the trial-and-error approach can be effective for small and simple networks in the hands of well-experienced engineers, this approach quickly becomes impossible as the network grows in both size and complexity. In modern cellular radio networks, due to the full frequency reuse as well as the large number of cells, it is difficult and time-consuming to optimize a cellular network to maximize a predefined performance metric. The joint optimization for the parameters of real cellular networks with irregular layouts and coverage areas has become a very complex task in practice.

To simplify the optimization task, typically each of the parameters is only allowed to take values from a finite set within a certain range, which is also a good reflection of the practice. Nevertheless, even with this simplification, the number of possible combinations is still prohibitively large for a brute-force search for the best solution. Therefore heuristic local search methods such as SA, GA, and Tabu search have been used. The major problem of these local search methods is that there is no guarantee for finding the global optimal solution and their performance is highly dependent on the heuristic selection of the initial values [10-13]. As a major improvement to the brute-force global search, recently an iterative optimization procedure using the Taguchi method has been proposed [13]. The advantage of TM is that it uses the OA to select a reduced set of representative parameters from the full search space to test, thus reducing the computational complexity greatly. The OA has a profound background in statistics

[22]. It provides an efficient and a systematic way to find the optimal result with only a few experimental runs in the full search space. In the TM-based optimization, the OA columns stand for different configuration parameters and the OA rows stand for different experiments that consider the interactions among these configuration parameters.

In practice, engineers always want to reduce the cost of optimization computation. A Nearly-Orthogonal Array (NOA) has been proposed to replace OA in order to further reduce the number of experiments [23]. NOA allows joint optimization of the configuration parameters as it offers more flexibility in the number of parameters and experiments, and it is easier to construct as compared to OA [23]. This thesis develops further the existing NOA method proposed with the following improvements. Firstly, it is proposed to use the mixed-level NOA instead of the identical-level NOA [24]. The mixed-level NOA enables the use of different number of levels for different configuration parameters that have different optimization ranges, thus providing a better coverage of the full search space. Secondly, an improved mapping function is introduced to achieve an even distribution of levels across the optimization range. Finally, a hybrid approach employing multiple mixed-level NOAs with descending number of levels is adopted in the iterative optimization procedure to significantly reduce the total number of experiments while still achieving similar optimization performance to that of a single identical-level NOA.

5.2 Cellular Network Optimization Problem in LTE-A

An LTE-A network consists of a number of cells operating in the same frequency spectrum with each cell providing coverage to a different area. Considering the antenna tilt Θ_c and azimuth orientation Φ_c of each cell c (=1, …, C) as the configuration parameters to be optimized, the total number of configuration parameters is $2C$. Let the variable x_t (where t = 1, …, $2C$) be the configuration parameters and let γ_c be any performance metric for cell c. Due to frequency reuse of one, a change to a configuration parameter of cell c affects not only the performance metric γ_c, but also the performance metrics of all other cells. Hence, the optimization problem is formulated to maximize the network optimization function $y(\gamma_1, \ldots, \gamma_C)$ as a joint function of the performance metrics of all cells by finding the optimal values of the configuration parameters [13]:

$$\{x_1^{(\text{opt})}, \ldots, x_{2C}^{(\text{opt})}\} = \underset{x_1,\ldots,x_{2C}}{\arg\max}\ y(\gamma_1, \ldots, \gamma_C). \qquad (5\text{-}1)$$

To evaluate the cell edge user performance in cell c, a common criterion is the five percentile (5%-tile) of the Cumulative Distribution Function (CDF) of the User Equipment (UE) throughput denoted as $\gamma_{c,5\%}$ [25]. Following [13], letting $\gamma_c = \gamma_{c,5\%}$ puts emphasis on optimizing cell coverage.

Normally, there are two averaging methods that have been used as optimization functions. The first is Arithmetic Mean (AM). The disadvantage of AM is that AM may alleviates the impact of a small $\gamma_{c,5\%}$ in a cell network and aggravates the impact of a large $\gamma_{c,5\%}$. So, the AM algorithm would probably converge to a solution that increases the mean of $\gamma_{c,5\%}$, which does not necessarily increase $\gamma_{c,5\%}$ in every cell c. The Harmonic Mean (HM) averaging methods always aggravates the impact of small $\gamma_{c,5\%}$ and lessens the impact of large $\gamma_{c,5\%}$ [13]. Obviously, HM is better than the AM in providing equitable user experience throughout the network. The optimization function as the HM of the cell performance metrics is given by [13]

$$y(\gamma_1, \ldots, \gamma_C) = \text{HM}(\gamma_{c,5\%}) = \frac{C}{\sum_{c=1}^{C} \frac{1}{\gamma_{c,5\%}}}. \qquad (5\text{-}2)$$

5.3 Procedure of Taguchi's Method by Using Multiple Mixed-Level NOAs

The iterative optimization procedure based on TM is introduced in [23]. In this section, the optimization procedure presented in [23] is modified to adopt multiple mixed-level NOAs instead of a single identical-level NOA, along with an improved mapping function rather than the existing mapping function.

The first step of the optimization procedure is to construct a set of mixed-level NOAs. As it will become clear at the end of Section 5.3.6, the parameter optimization range, number of parameter levels, reduction factor and termination criterion decide the number of iterations in the optimization. The number of experiments in an iteration is determined by the NOA employed, and it generally increases with the number of levels. The proposed hybrid approach is employing several mixed-level NOAs through the whole optimization procedure. Because the reduction factor decreases the parameter range as the number of iterations increases, the number of levels can be reduced to cut the number of experiments. In the hybrid approach, the first mixed-level NOA has the

largest number of experiments, and each succeeding mixed-level NOA has smaller number of levels and hence less experiments. The iteration scheme is to split the total number of iterations among several mixed-level NOAs. If the first mixed-level NOA takes more iterations, it will generally lead to a better optimization result. If the last mixed-level NOA takes more iterations, the procedure will require a smaller total number of experiments. At the beginning of each iteration, a mapping function is employed to select testing values for each parameter according to the number of levels available in the NOA. Taguchi's method is then applied to obtain performance figures of all the combinations as defined by the mixed-level NOA. The performance figures are then processed and checked against the termination criterion. If the termination criterion is met, the optimization ends. If not, the optimization range is reduced based on the current results obtained and the optimization moves onto the next iteration. The process continues until the termination criterion is satisfied. The flowchart of the improved iterative optimization procedure is shown in Figure 5-1, with each major step detailed in the following.

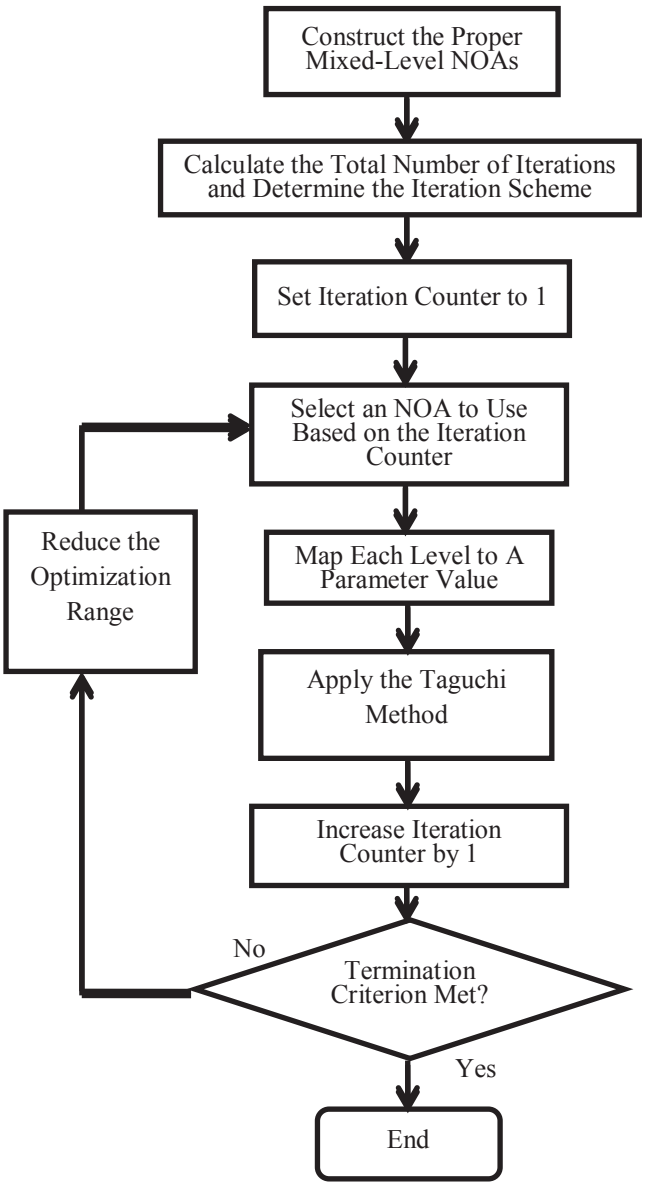

Figure 5-1: Flowchart of the improved TM-based iterative optimization procedure using multiple mixed-level NOAs

5.3.1 Construct the Proper Mixed-Level NOAs

OA is an array containing a reduced set of N parameter combinations to be tested from the full search space [22]. Each parameter has a set of levels. A set of levels is mapped to a set of values of each parameter. Every combination i (= 1, …, N) determines an experiment that has a measured response y_i. OA has been used in industries for

productivity and quality improvement experiments. However, its use in cellular network optimization is only a recent development. As more experiments mean more cost and time, it is desirable to reduce the number of experiments as much as possible. However, the minimum number of experiments determined by OA is bounded by the number of parameters and the number of levels [22]. When the number of parameters is large, the number of experiments required by OA may become computationally impossible. A good solution is to use NOA instead of OA. NOA is easier to be constructed for any number of parameters and any number of experiments, and it allows mixed-level parameters, that is, different parameters may have different number of levels [24].

The existing method employs identical-level NOA, which only allow the same number of levels for any configuration parameters being optimized. Table 5-1 shows an example of the identical-level NOA (6, 4, 3), which has $N = 6$ combinations, 4 parameters with each parameter having 3 different levels.

Table 5-1: Illustrative identical-level NOA (6, 4, 3) with the measured responses and their corresponding SN ratios

Experiment	x_1	x_2	x_3	x_4	Measured Response	SN Ratio
1	1	1	1	3	y_1	SN_1
2	1	2	3	2	y_2	SN_2
3	2	3	2	1	y_3	SN_3
4	2	1	2	3	y_4	SN_4
5	3	2	3	2	y_5	SN_5
6	3	3	1	1	y_6	SN_6

In this thesis, we consider the optimization of two types of configuration parameters: antenna tilt and azimuth orientation. Thus, the total number of configuration parameters for a network of C cells is $2C$. The azimuth orientation parameters typically have a large dynamic range. Hence a sufficiently large number of levels are necessary to enable representative testing of the full range with good resolution. In contrast, the antenna tilt parameters have a small range and need only a small number of levels for sufficient resolution. The advantage of tailoring the number of levels according to the parameter range is that, by removing unnecessary levels, the number of experiments can be reduced without affecting the optimization performance. To allow different number of levels for different types of configuration parameters in the joint optimization, mixed-

level NOA [24] can be used. This is in contrast to the identical-level NOA employed in [23], where different types of configuration parameters must have the same number of levels. Table 5-2 shows an example of the mixed-level NOA (6, 3^2, 2^2) having $N = 6$ combinations and 4 configuration parameters. The notation 3^2 means that the first 2 parameters have $s = 3$ levels, while 2^2 means that the rest 2 parameters have $s = 2$ levels. Each level represents a different value within the range of the parameter, as determined by the mapping function. In the optimization, the mixed-level NOA approach achieves better optimization results than the identical-level NOA. More details are presented in Chapter 6 on simulation results. An effective algorithm for constructing mixed-level NOA is described in [24].

Table 5-2: Illustrative mixed-level NOA (6, 3^2, 2^2) with the measured responses and their corresponding SN ratios

Experiment	x_1	x_2	x_3	x_4	Measured Response	SN Ratio
1	1	1	1	1	y_1	SN_1
2	1	2	1	2	y_2	SN_2
3	2	3	2	1	y_3	SN_3
4	2	1	2	2	y_4	SN_4
5	3	2	1	1	y_5	SN_5
6	3	3	1	2	y_6	SN_6

5.3.2 Determine the Iteration Scheme

To implement the proposed hybrid approach employing several mixed-level NOAs for further reduction in computational complexity, an iteration scheme is needed to determine how these NOAs are used through the whole optimization procedure. For example, assuming that there are 10 iterations in the whole optimization procedure, in the first 3 iterations the mixed-level NOA (32, 8^2, 6^2) is used; in the subsequent 4 iterations NOA (24, 6^2, 4^2) is employed, reducing the number of levels from 8 and 6 to 6 and 4, respectively; and in the last 3 iterations NOA (16, 4^2, 2^2) is used with further reduction in the number of levels. Thus, the total number of experiments in 10 iterations with the proposed hybrid approach is $32 \cdot 3 + 24 \cdot 4 + 16 \cdot 3 = 240$. The iteration scheme in this example can be denoted as 3-4-3. If the mixed-level NOA (32, 8^2, 6^2) is used throughout all of the optimization iterations, it will take $32 \cdot 10 = 320$ experiments.

Hence, in this example the hybrid approach achieves a 25% reduction in computational complexity as compared to the single-NOA approach.

5.3.3 Map Each Level to A Parameter Value

In the first iteration m = 1, the centre value of the optimization range for parameter x_t is defined as

$$V_t^{(m)} = \frac{\min_t + \max_t}{2} \tag{5-3}$$

where $\min_t$ and $\max_t$ are the minimum and maximum feasible values for parameter x_t, respectively. The s is number of levels for dynamic range. The level values are distributed around $V_t^{(m)}$ by subtracting or adding the Level Difference (LD) [26] proportionally according to the mapping functions defined below. In the first iteration the LD for parameter x_t is given as

$$LD_t^{(m)} = \frac{\max_t - \min_t}{s+1} \tag{5-4}$$

In iteration m, the parameter value for level l is calculated from the mapping function $f_t^{(m)}(l)$. When s is an odd number, the mapping function is defined as [23]

$$f_t^{(m)}(l) = \begin{cases} V_t^{(m)} - (\lceil s/2 \rceil - l) \cdot LD_t^{(m)} & 1 \le l \le \lceil s/2 \rceil - 1 \\ V_t^{(m)} & l = \lceil s/2 \rceil \\ V_t^{(m)} + (l - \lceil s/2 \rceil) \cdot LD_t^{(m)} & \lceil s/2 \rceil + 1 \le l \le s \end{cases} \tag{5-5}$$

However, when s is an even number, the mapping function is defined as follows

$$f_t^{(m)}(l) = \begin{cases} V_t^{(m)} - (s/2 - l + 1/2) \cdot LD_t^{(m)} & 1 \le l \le s/2 \\ V_t^{(m)} + (l - s/2 - 1/2) \cdot LD_t^{(m)} & s/2 < l \le s \end{cases} \tag{5-6}$$

The mapping functions defined in (5-5) and (5-6) distinguish between odd and even number of levels, with the aim to distribute parameter levels evenly over the optimization range. This is an improvement to the existing mapping function in [23], where (5-5) was used in existing method for any values of s. As an example, if the antenna azimuth orientation optimization range is from -15° to 15°, and the number of levels is s=5, then in the first iteration m=1, the centre value is $V_t^{(1)} = \frac{-15+15}{2} = 0$, and the level difference is $LD_t^{(1)} = \frac{15-(-15)}{5+1} = 5$. Using the existing mapping function (5-5),

we have $f_t^{(1)}(1) = -10$, $f_t^{(1)}(2) = -5$, $f_t^{(1)}(3) = 0$, $f_t^{(1)}(4) = 5$, and $f_t^{(1)}(5) = 10$. From Figure 5-2, we can see that the levels are evenly distributed over the optimization range.

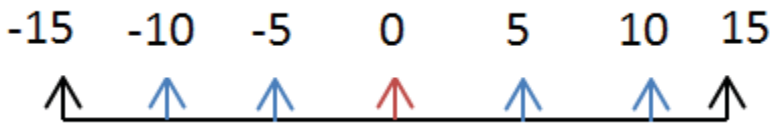

Figure 5-2: Example for odd *s*

In contrast, for the mapping of s = 4 levels for the antenna tilt parameter with an optimization range from 0^o to 10^o in the first iteration, the existing mapping function defined in (5-5) gives the following mapping: level 1= 3, level 2= 5, level 3= 7 and level 4= 9. Obviously, the level values are not evenly distributed over the entire range. However, the result of mapping function (5-6) is: level 1= 2, level 2= 4, level 3= 6 and level 4= 8, which distributes the levels evenly across the parameter range. Figure 5-3 shows the two different results from these two mapping functions, respectively. Therefore, regardless the number of levels, the improved mapping function always selects representative values from the optimization range with uniform spacing, and thus is expected to achieve better optimization results. This is verified by simulation results presented in Chapter 6.

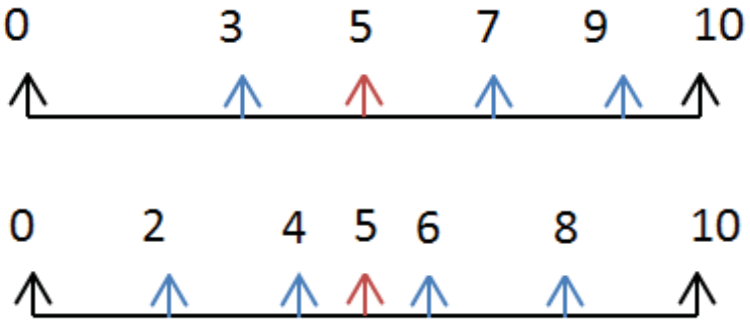

Figure 5-3: Results of two mapping functions when *s* is even

5.3.4 Apply Taguchi's Method

After conducting all the N experiments, the Taguchi method converts the experiment result of each parameter combination using signal-to-noise (SN) ratios. SN ratio for each combination i is given by [13]

$$\mathrm{SN}_i = 10\log_{10}(y_i^2)[\mathrm{dB}] \tag{5-7}$$

After computing SN_i for each combination i, the highest average SN ratio determines the best level $l_t^{(\mathrm{best},m)}$ for each parameter x_t. The average SN ratio of x_t at level l is calculated as

$$\overline{\mathrm{SN}}_{l,t} = \frac{1}{N_{t,l}} \sum_{i|\mathrm{NOA}_{(i,t)}=l} \mathrm{SN}_i \tag{5-8}$$

where $\mathrm{NOA}_{(i,t)}$ is the testing level of parameter x_t in experiment i, and $N_{t,l}$ is the number of experiments with x_t at level l. Using Table 5-2 as an example, the average SN ratio of parameter x_2 at level 1 is $(\mathrm{SN}_1+\mathrm{SN}_4)/2$. After calculating the average SN ratio for every level, the best level is the level that has the highest average SN ratio. That is, the best level $l_t^{(\mathrm{best},m)}$ for each parameter x_t is computed as

$$l_t^{(\mathrm{best},m)} = \arg\max_{l} \overline{\mathrm{SN}}_{l,t} \tag{5-9}$$

The parameter value associated with the best level is the best value found for x_t in the current iteration m and is denoted as $V_t^{(\mathrm{best},m)}$.

5.3.5 Shrink the Optimization Range

The best values found from iteration m are used as the centre values in iteration m+1:

$$V_t^{(m+1)} = V_t^{(\mathrm{best},m)} \tag{5-10}$$

Also, the LD is reduced by a reduction factor $\xi < 1$ as follows

$$LD_t^{(m+1)} = \xi \cdot LD_t^{(m)} \tag{5-11}$$

The LD reduction effectively shrinks the optimization range. A higher value of ξ makes the convergence of the algorithm slower, but the optimization more accurate. A lower value of ξ shrinks the optimization range faster, at the expense of a possible degradation in performance. The level values $f_t^{(m+1)}(l)$ are updated according to (5-5) and (5-6).

There is a need for a procedure to ensure that the updated level values are within the optimization range. For example, if $f_t^{(m+1)}(s)$ is large than $\max_t$, the mapped values of levels from $\lceil s/2 \rceil + 1$ or $s/2$ to s are distributed such that they are equally spaced between $V_t^{(m+1)}$ and $\max_t$.

Furthermore, with the proposed hybrid approach using multiple mixed-level NOAs, every switching of NOA represents a reduction in the number of levels, which in general accelerates the shrink of the optimization range by a factor β = ratio of the current number of levels to the initial number of levels. Considering the example NOAs in Section 5.3.2, when switching from NOA (32, 8^2, 6^2) to NOA (24, 6^2, 4^2), the factor for shrink acceleration is approximately 6/8 = 3/4 and 4/6 = 2/3 for the first two parameters and the last two parameters, respectively. An accurate analysis on the shrinkage of optimization range is presented in Section 5.5.

5.3.6 Check the Termination Criterion

As the optimization range shrinks with the LD reduction and NOA switching, eventually all level values become close to each other. The optimization procedure is terminated when differences between the level values are too small to make notable differences in SN ratios. Therefore a convenient measure that can be used in the termination criterion is $LD_t^{(m)}$ and we define the termination criterion as follows

$$LD_t^{(m)} < \epsilon \cdot LD_t^{(1)}, \forall t\,, \tag{5-12}$$

where ϵ is typically small, e.g., 0.01 or 1%, depending on the initial value of the LD and the practical adjustment precision of the configuration parameter.

5.4 LTE-A System Model

In this section, the downlink system model of an LTE-A cellular network tested by the proposed optimization procedure is presented. System-level simulations are used to carry out the experiments to generate performance metrics needed in the optimization.

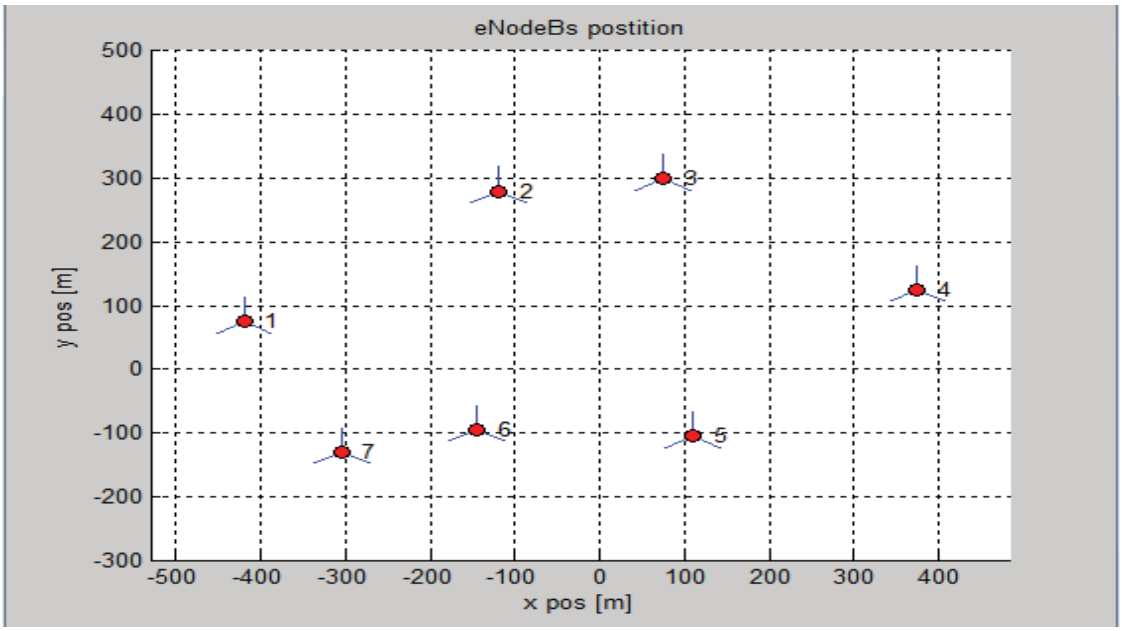

Figure 5-4: LTE-A network with cells of different coverage areas and default azimuth orientations

5.4.1 General Definitions

The LTE-A network has $k = 7$ enhanced NodeBs (eNodeBs) with $C = 21$ cells located in a 1000×800 m^2 area as shown in Fig. 5-4. Each cell is served by an eNodeB sector. The system bandwidth is 10 MHz with 50 Physical Resource Blocks (PRBs). The maximum eNodeB transmission power is 40 W per PRB. The path loss is set according to the path loss model for the Urban Macro (Uma) None-Line-of-Sight (NLoS) scenario provided in [27]. Map resolution is 5 meters per pixel. The shadow fading standard deviation is set to 6 dB and the inter-site shadow fading correlation is 0.5. The receiver noise figure is 7 dB and the thermal noise density is -174 dBm per Hz. The eNodeB antenna height is 25 m and the UE height is 1.5 m. The 3-Dimensional (3D) eNodeB antenna pattern is adapted based on the popular Kathrein 742215 antenna model parameters [28-29]. Note that the maximum antenna backward attenuation B_0, the azimuth beam width $\Delta_{\emptyset}$, and the elevation beam width Δ_{θ} are set the same as those used in [23]. The antenna model and parameters are summarized in Table 5-3, where $\emptyset$ and θ are azimuth and elevation angles, respectively, of the line-of-sight between UE and eNodeB. The LTE-A system model general definitions are summarized in Table 5-4.

Table 5-3: Antenna model and parameters

Parameter	Model
Azimuth pattern	$B_{\emptyset}(\emptyset) = -\min\left\{B_0, 12\left(\frac{\emptyset - \Phi}{\Delta_{\emptyset}}\right)^2\right\}$ $B_0 = 25$ dB, $\Delta_{\emptyset} = 70^{o}$ and Φ: azimuth orientation
Elevation pattern	$B_{\theta}(\theta) = -\min\left\{B_0, 12\left(\frac{\theta - \Theta}{\Delta_{\theta}}\right)^2\right\}$ $B_0 = 25$ dB, $\Delta_{\theta} = 9^{o}$ and Θ: tilt
3D antenna pattern	$\mathrm{B}(\emptyset, \theta) = -\min\{-[B_{\emptyset}(\emptyset) + B_{\theta}(\theta)], B_0\}$
Antenna gain	17 dBi

Table 5-4: LTE-A system model general definitions

General Definitions	
Cells: 7 eNodeBs (random position), 21 sectors	
Frequency (f_c): 2 GHz	Transmit power: 40 W
Bandwidth: 10 MHz with 50 Physical Resource Blocks (PRBs)	
UE receiver noise figure: 7 dB	Thermal noise: -174 dBm/Hz
UE height (h_{UT}) is 1.5 m	Map resolution: 5 m
Antenna model: 3-D Kathrein 742215 antenna model	
Antenna max gain: 17 dBi	Antenna height (h_{BS}): 25 m
The shadow fading standard deviation: 6 dB	
Shadow fading correlation: 0.5	

Pathloss model: PL = 161.04 – 7.1 $\log_{10}(W)$ + 7.5 $\log_{10}(h)$– (24.37 – 3.7$(h/h_{BS})^2$) $\log_{10}(h_{BS})$+ (43.42 – 3.1 $\log_{10}(h_{BS})$) ($\log_{10}(d)$ − 3) +20 $\log_{10}(f_c)$ – (3.2 ($\log_{10}$ (11.75 h_{UT}))^2 − 4.97).

h = average building height = 20 m, W = average street width = 20 m.

5.4.2 Calculation of UE Throughput

We consider that each UE is served by one PRB. A full load system where every UE is affected by all other neighboring antennas is assumed in the calculation of the Signal-to-Interference-Noise Ratio (SINR). The downlink throughput R of a UE can be approximated using Shannon's equation as

$$R = W_{\text{eff}} \cdot B \cdot \log_2\left(1 + \frac{\text{SINR}}{S_{\text{eff}}}\right) \text{ [kbps]}, \qquad (5\text{-}13)$$

where S_{eff} =1.25 is the SINR efficiency factor and W_{eff} = 0.88 is the bandwidth efficiency factor [30]. The bandwidth of a PRB is B = 180 kHz.

5.5 Optimization Range Shrink Analysis

Due to the LD reduction factor ξ which is less than 1, the LD decreases according to (5-11) after each iteration. Loosely speaking, the optimization range decreases at the same speed as the LD decreases. It is easy to see that the LD in the mth iteration can be written as

$$LD_t^{(m)} = \xi^{m-1} \cdot LD_t^{(1)}. \qquad (5\text{-}14)$$

Therefore, the amount of LD reduction in iteration m as compared to iteration 1 in percentage is given by

$$\left(LD_t^{(1)} - LD_t^{(m)}\right)/LD_t^{(1)} \times 100\% = \left(1 - \xi^{m-1}\right) \times 100\%. \qquad (5\text{-}15)$$

That is, the LD reduction percentage is a function of the iteration number m. For instance, the curve of the LD reduction percentage versus the iteration number is plotted in Fig. 5-5 for $\xi = 0.8$. As can be observed from the figure, the LD reduction is fast in the first few iterations. However, as the iteration continues, it starts to level off towards

the vicinity of 1. Comparing (5-14) with (5-12), it can be seen that the total number of iterations *M* is determined by

$$M = \left\lceil \frac{\log \epsilon}{\log \xi} + 1 \right\rceil. \tag{5-16}$$

Alternatively, observing the optimization range shrink as a percentage of the original optimization range in iteration 1, the range shrinkage made in the second iteration is $20\% = 1 - \xi$; and in the third iteration the optimization range is shrunk to 64%, thus the shrinkage made in the iteration is $16\% = (1 - \xi)\xi$. Generalizing this observation, the shrinkage made in iteration *m* is found to be $(1 - \xi)\xi^{m-2}$, and the total shrinkage at iteration *m* is given by

$$\sum_{i=2}^{m}(1 - \xi)\xi^{i-2} = 1 - \xi^{m-1}. \tag{5-17}$$

Clearly, (5-17) is equivalent to (5-15).

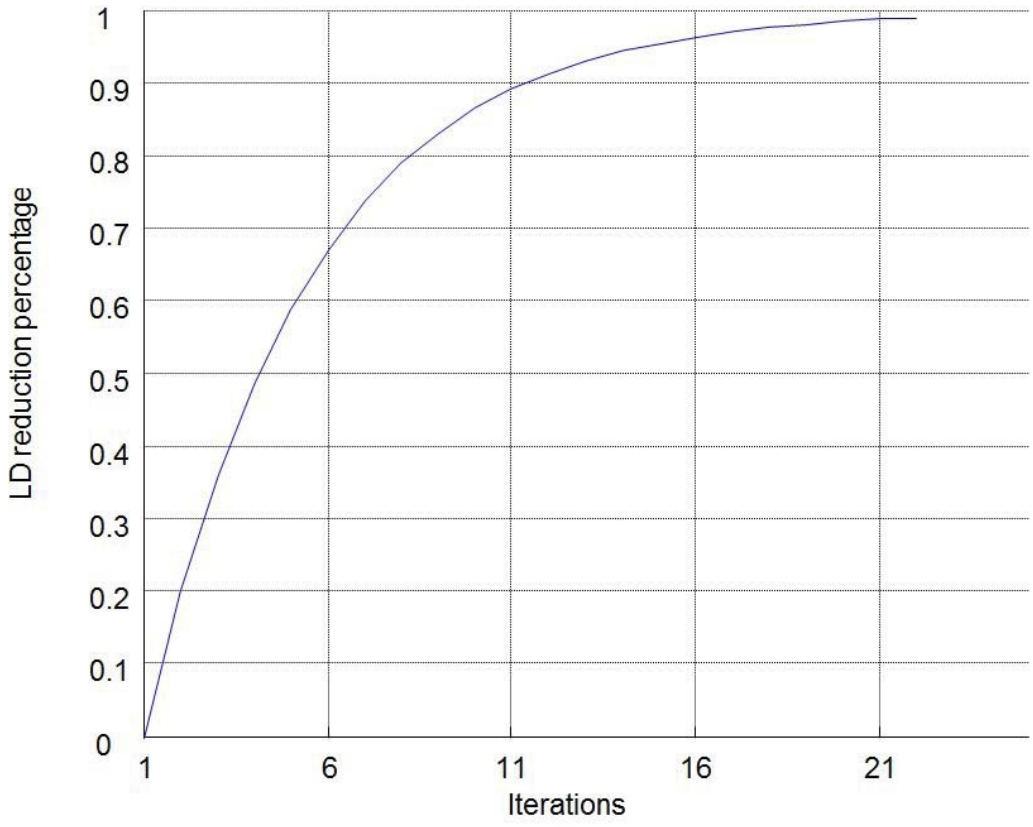

Figure 5-5: LD reduction percentage in 22 iterations when the reduction factor is 0.8

The analysis above is based on the assumption of using a single OA or NOA in all the iterations, where the number of levels does not change. When multiple NOAs are used, this analysis needs to be modified to consider the reduction of the number of levels due to NOA switching. To make it easy to understand, an example is used in the following discussion. Assuming that the reduction factor is $\xi = 0.8$ and the termination criterion is $\epsilon = 0.01$, then from (5-16) the total number of iterations is $M = 22$. If NOA (64, 21, 8) is used in all 22 iterations, then the total optimization range shrinkage at an iteration is identical to the LD reduction percentage, which is the same as that shown in Figure 5-5. However, if NOA (64, 21, 8) is only used in the first 5 iterations, and NOA (42, 21, 6) is used in the rest 17 iterations, then due to NOA switching at iteration 6, where the number of levels is reduced from 8 to 6, the optimization range is shrunk to $(6+1)LD_t^{(6)}$ instead of $(8+1)LD_t^{(6)}$. That is, in iteration 6, besides the usual shrinkage of $(1-\xi)\xi^{6-2}$, there is an additional reduction of $2LD_t^{(6)} = 2\xi^{6-1} \cdot LD_t^{(1)}$, or $(2/9)\xi^{6-1}$ as a percentage of the original optimization range of $(8+1)LD_t^{(1)}$ in iteration 1. Similar shrinkage can also be observed in subsequent iterations. Therefore, generalizing the above discussion, the total optimization range shrinkage at iteration m, with two NOAs where the first NOA has L_1 levels and is used in the first M_1 iterations, while the second NOA has L_2 ($< L_1$) levels and is used in the rest $M-M_1$ iterations, is given by

$$\sum_{i=2}^{m}(1-\xi)\xi^{i-2} + \frac{L_1 - L_2}{L_1 + 1}\sum_{i=M_1+1}^{m}\xi^{i-1} = \left(1-\xi^{m-1}\right) + \frac{L_1 - L_2}{L_1 + 1}\cdot\frac{1-\xi^{m-M_1}}{1-\xi}\xi^{M_1} \tag{5-18}$$

From (5-18), it can be seen that the extra shrinkage in optimization range increases as L_1-L_2 increases, or as M_1 decreases. Hence, in the case of multiple NOA, the optimization range shrink is faster than the LD reduction. For comparison, the total optimization range shrinkage versus the iteration number is plotted for both the single-NOA case and the two-NOA case of the above example in Figure 5-6, respectively. Note that the faster the optimization range shrinks, the faster the optimization converges. It is also worth pointing out that the total number of experiments decreased from $64 \cdot 22 = 1408$ for the single-NOA case to $64 \cdot 5 + 42 \cdot 17 = 1034$ for the two-NOA case.

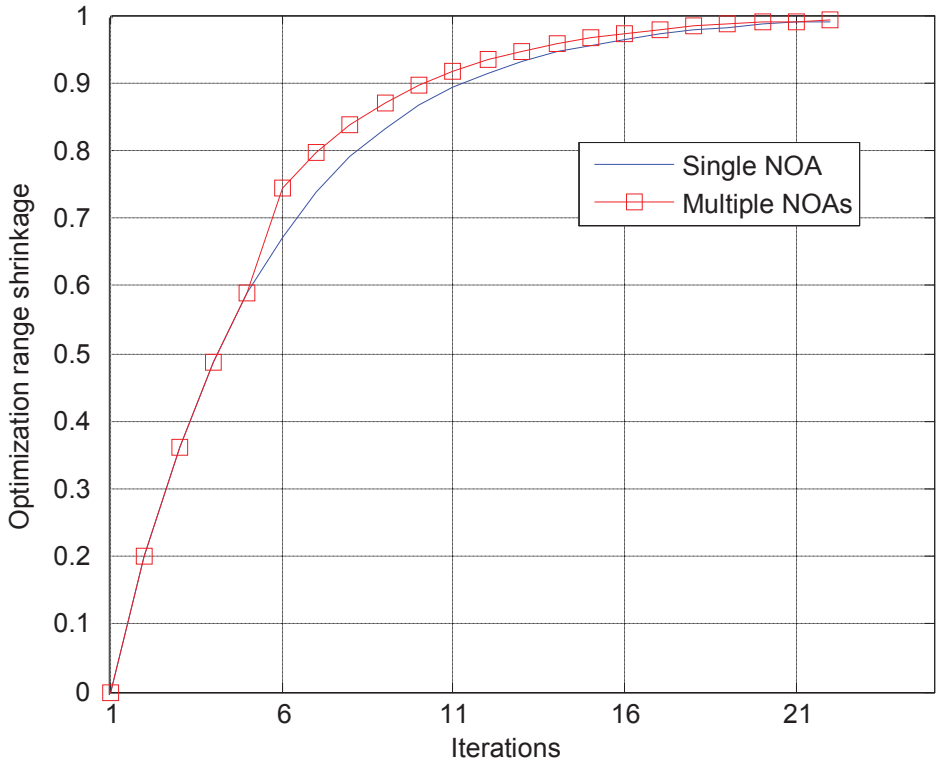

Figure 5-6: Comparison of total optimization range shrinkage between the single-NOA case and the two-NOA case in 22 iterations when the reduction factor is 0.8

6 Simulation Results

Results of the joint optimization using the proposed mixed-level NOA with improved mapping function and the proposed hybrid approach with multiple mixed-level NOAs are presented and compared with that of the existing approach [23] with a single identical-level NOA.

6.1 Algorithm Parameters

Every eNodeB has three sectors. The default parameter setting for the azimuth orientation is $\{0^o, \pm 120^o\}$ and the tilt is 6^o. Hence the azimuth orientation Φ ranges from -59^o to 59^o with respect to its default setting. The tilt Θ ranges from 0^o to 10^o. The reduction factor ξ is set to 0.8 and termination criterion ϵ is set to 0.01.

6.2 Improved Mixed-level NOA versus Identical-level NOA

The azimuth orientation has an optimization range of 118^o and the tilt has an optimization range of 10^o. With the same number of experiments, using mixed-level NOA for joint optimization would allow more tests for parameters having smaller number of levels. The existing identical-level NOA approach uses only mapping function (5-5) and the same number of levels for all parameters. The improved mixed-level NOA uses mapping functions (5-5) & (5-6) to distribute parameter levels evenly over the optimization range so that the probability of missing the near-optimal solution is reduced. Figure 6-1 shows the optimization results of using the identical-level NOA (96, 42, 8) and the improved mixed-level NOA (96, 8^21, 6^21). The results are the $\mathrm{HM}(\gamma_{c,5\%})$ calculated using (5-2), which focus on the 5%-tile of the UE throughput distribution. The HM ($\gamma_{c,5\%}$) achieved by the mixed-level NOA is 129 kbps, while the identical-level NOA attains 125 kbps. Therefore, the proposed mixed-level NOA has better performance than the existing identical-level NOA. Note that both methods have the same number of iterations and the same number of experiments, hence the same computational complexity.

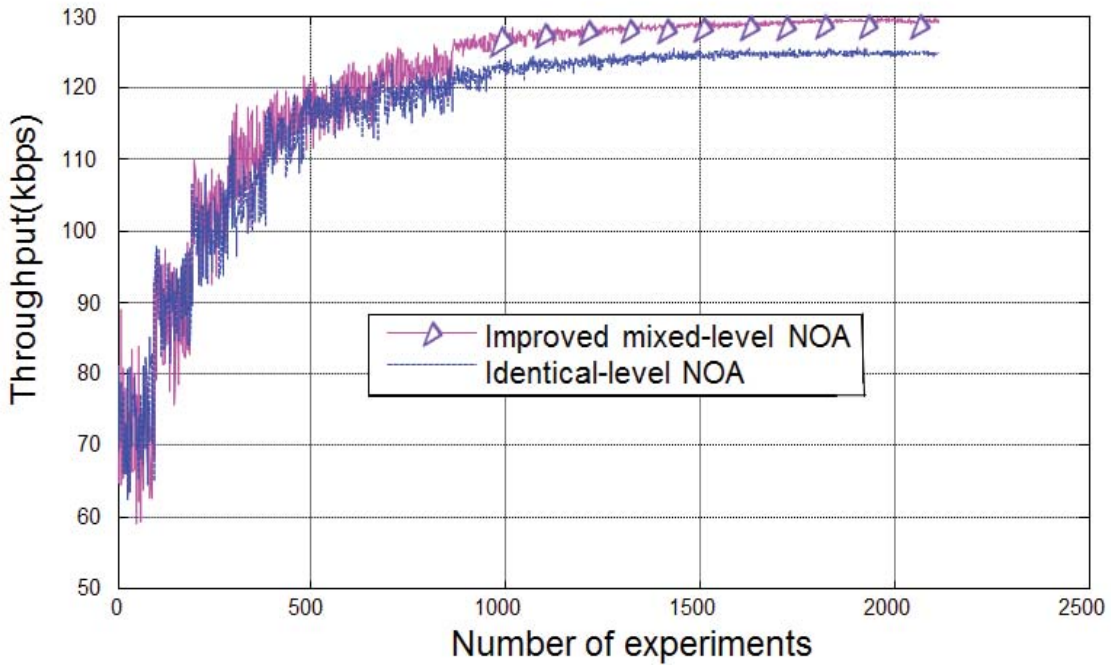

Figure 6-1: Comparison of optimization performance between improved mixed-level NOA and identical-level NOA

6.3 Hybrid Approach Using Multiple Mixed-Level NOAs

The proposed hybrid approach uses multiple mixed-level NOAs in the optimization procedure instead of the single mixed-level NOA used in Section 6.2, while keeping the same number of iterations. By switching to NOA with smaller number of levels and hence smaller number of experiments during the optimization iterations, the total number of experiments can be reduced significantly with little degradation in optimization performance. In this simulation the hybrid approach uses NOA (96, 8^21, 6^21), NOA (60, 5^21, 4^21), and NOA (36, 3^21, 2^21) in tandem in the optimization iteration. Defining the accuracy metric as the minimum number of experiments that each level is tested in one iteration for any parameter, it can be seen that all the above three NOAs have the same accuracy metric because $96/8 = 60/5 = 36/3 = 12$. As the antenna azimuth orientation has a much larger optimization range than that of the antenna tilt, it is assigned more levels than the tilt. With the reduction factor $\xi = 0.8$ and termination criterion $\epsilon = 0.01$, we can calculate that the total number of iterations is 22. The optimization iteration begins with NOA (96, 8^21, 6^21), where each of the 21 parameters for azimuth orientation has 8 levels, and the tilt has 6 levels. After M_1 iterations, NOA (60, 5^21, 4^21) takes over and reduces the number of levels, which

leads to reduced number of experiments. After another M_2 iterations, NOA (36, 3^21, 2^21) kicks in to further reduce the number of experiments. The optimization iteration terminates after a further M_3 iterations. Thus, with the total number of iterations = $M_1+M_2+M_3$ = 22, the hybrid approach has a total number of experiments = $96M_1+60M_2+36M_3$, while the single-NOA approach using NOA (96, 8^21, 6^21) in all of the 22 iterations has a total of $96 \cdot 22 = 2112$ experiments. For convenience, we denote a specific iteration scheme as $M_1-M_2-M_3$. Switching from the first NOA (96, 8^21, 6^21) to the second NOA (60, 5^21, 4^21), the optimization range shrinks to $(L_2 + 1) \cdot LD_t^{(M_1+1)}$ instead of $(L_1 + 1) \cdot LD_t^{(M_1+1)}$. When switching to the third NOA (36, 3^21, 2^21), the optimization range shrinks to $(L_3 + 1) \cdot LD_t^{(M_1+M_2+1)}$. In the above, L_1, L_2 and L_3 denote the largest number of levels in three NOAs, respectively.

6.4 Results of the Proposed Approaches

Figure 6-2 shows the results of 5%-tile SINR CDF F(x) optimization by using the identical-level NOA (96, 42, 8) and mixed-level NOA (96, 8^21, 6^21) with the existing mapping function, respectively, and the improved mixed-level NOA (96, 8^21, 6^21) where the improved mapping function is employed. As a reference, the CDF of the default parameter setting with azimuth orientation at $\{0^o, \pm 120^o\}$ and tilt at 6^o is also shown. From Figure 6-2 it is obvious that optimization of radio network parameters can significantly enhance network performance. It is easy to observe that with the existing mapping function, mixed-level NOA gives better result than identical-level NOA. Furthermore, the best result is achieved by the improved mixed-level NOA. Hence, Figure 6-2 shows that both the mixed-level NOA and the improved mapping function help to enhance the optimization result.

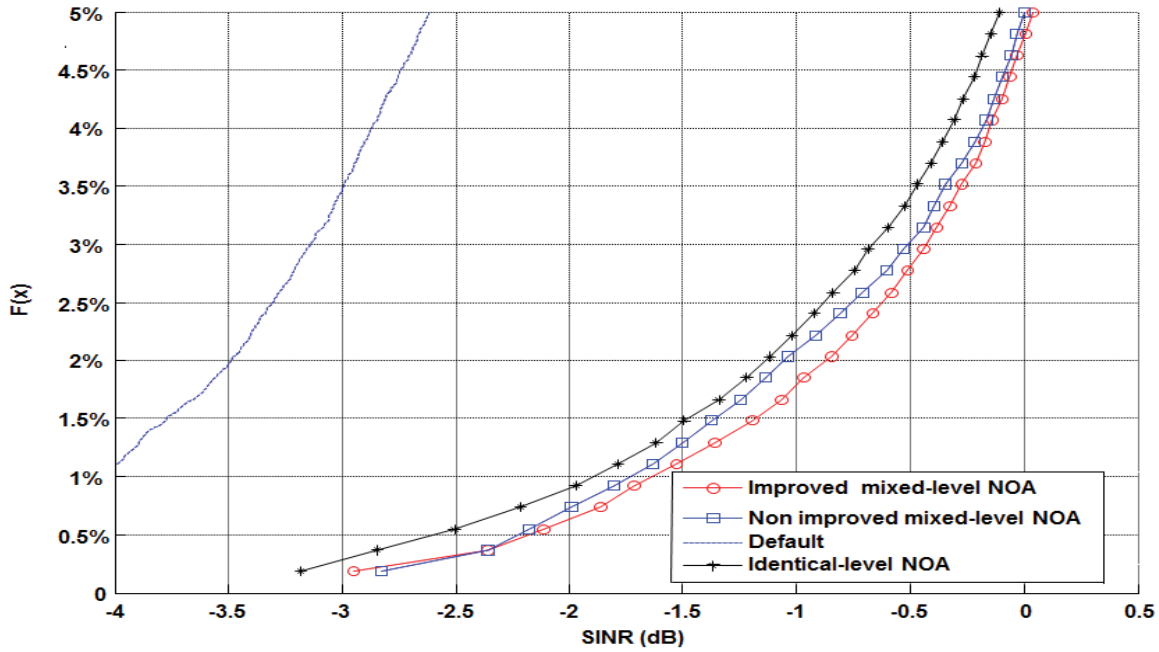

Figure 6-2: Comparison of optimized 5%-tile SINR CDFs between improved mixed-level NOA, mixed-level NOA, and identical-level NOA

Figure 6-3 shows optimized SINR CDFs F(x) of two mixed-level NOAs, NOA (96, 8^21, 6^21) and NOA (72, 8^21, 6^21), of different computational complexity, using the existing mapping function. With the same number of iterations, both mixed-level NOAs give better result than the identical-level NOA (96, 42, 8). The mixed-level NOA (96, 8^21, 6^21) has 96 experiments per iteration and provides only a small gain at the 5%-tile SINR than the mixed-level NOA (72, 8^21, 6^21) that has 72 experiments per iteration. Hence, fewer experiments in optimization iteration only incur a little penalty in optimization performance. In other words, we can save more experiments in the simulation, but obtain almost the same result that is better than the existing method based on the identical-level NOA (96, 42, 8).

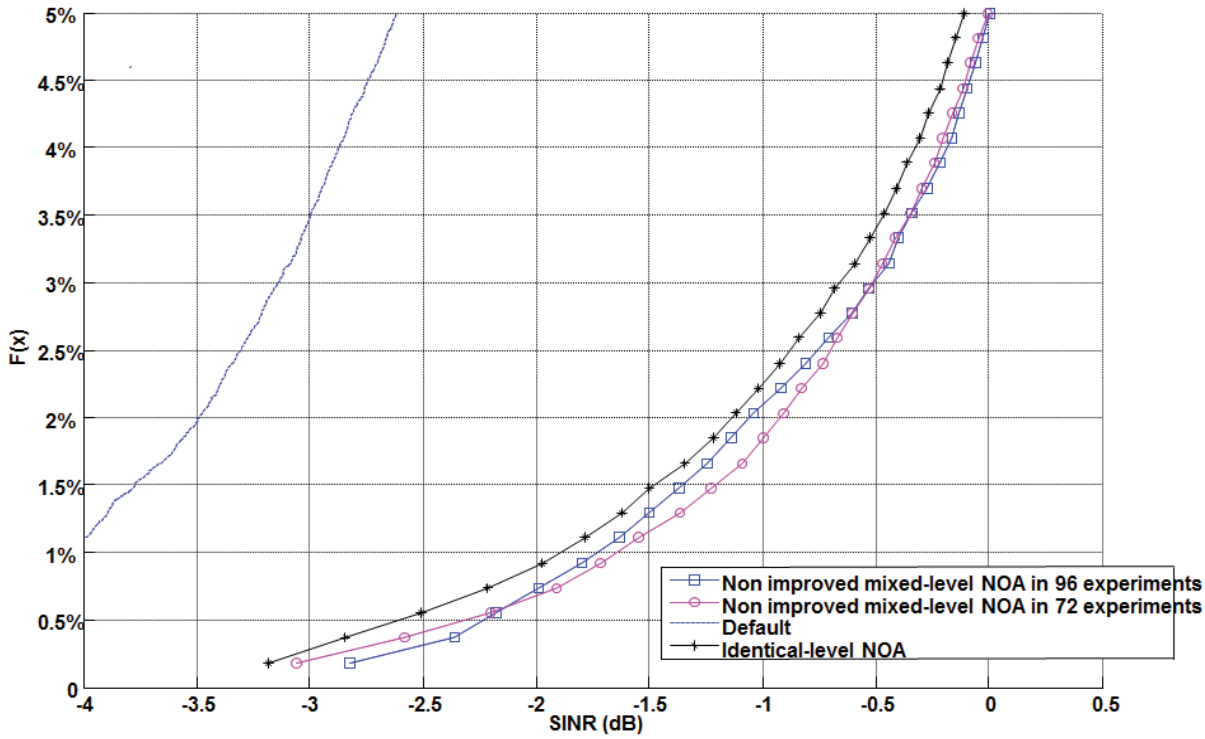

Figure 6-3: Comparison of optimized 5%-tile SINR CDFs of mixed-level NOAs having 96 experiments and 72 experiments per iteration, respectively

Table 6-1: Iteration schemes for the hybrid approach

Iteration Scheme	NOA employed	Total number of experiments	Percent of experiments saved
22 iterations using the same NOA	NOA (96, 8^21, 6^21)	2112	0
(5 – 4 – 13)	NOA (96, 8^21, 6^21), NOA (60, 5^21, 4^21), NOA (36, 3^21, 2^21)	1188	44%
(3 – 3 – 16)		1044	50%
(1 – 6 – 15)		996	53%

Using the identical-level NOA approach as the benchmark, three iteration schemes of the hybrid approach as listed in Table 6-1 are tested for optimization performance

comparison: 5-4-13, 3-3-16, and 1-6-15. It is easy to see that these three schemes can reduce the total number of experiments by approximately 44%, 50%, and 53%, respectively, as compared to the benchmark. The optimization results of the three schemes are compared with the benchmark using the 5%-tile SINR CDF F(x) of the 7-eNodeB network in Figure 6-4, where the CDF of the existing approach [18] using the identical-level NOA (96, 42, 8) is included. It confirms that with the same computational complexity, the proposed mixed-level NOA together with the improved mapping function yields better results than the identical-level NOA does. By using multiple NOAs with different number of experiments, the proposed hybrid approach allows the flexibility in computational complexity and optimization performance trade-off. As seen in Figure 6-4, significant reductions in computational complexity are achievable with only small degradations in optimization performance.

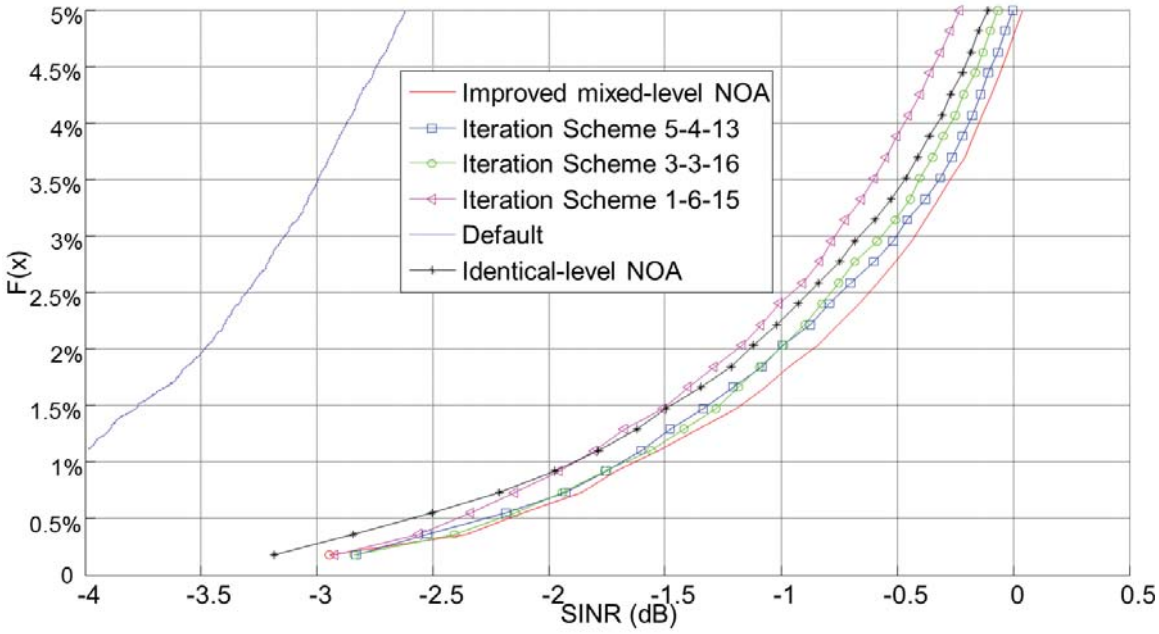

Figure 6-4: Optimized 5%-tile SINR CDFs of the hybrid approach

7 Conclusions and Future Work

The improved mixed-level NOA optimization procedure based on TM has been proven a valuable means for enhancing LTE-A network performance. The joint optimization of antenna parameters focuses on cell coverage and capacity maximization to enhance UE throughput. In this thesis, we have proposed the use of mixed-level NOAs and an improved mapping function in TM-based joint optimization of LTE-A radio network parameters to achieve better optimization performance than the existing method. To cut more experiments in the optimization procedure, we have developed a hybrid approach using multiple NOAs instead of a single NOA in the optimization. The hybrid approach uses multiple NOAs with successively decreasing number of experiments to reduce significantly the computational complexity with little sacrifice in optimization performance, making TM-based method attractive to optimizing practical networks. It can easily control the number of experiments to achieve the SINR target in the LTE-A network. A real cellular network is usually very big and complex. We have presented optimization results of small-scale networks using the proposed hybrid approach. Future work will investigate extending the proposed optimization approach to large-scale networks and jointly optimizing more parameters such as transmission power in addition to antenna azimuth orientation and tilt.

References

1. wiseGEEK, “What is 4G Mobile Technology?” [Online]. Available: http://www.wisegeek.com/what-is-4g-mobile-technology.htm
2. Radio-Electronics.com, “4G LTE Advanced Tutorial,” [Online]. Available: http://www.radio-electronics.com/info/cellulartelecomms/4g/3gpp-imt-lte-advanced-tutorial.php
3. E. Dahlman, S. Parkvall, and J. Skold, *4G LTE/LTE-Advanced for Mobile Broadband*. Elsevier, 2011.
4. M. Sauter, *Beyond 3G - Bringing Networks, Terminals and the Web Together*. Wiley, 2009.
5. “Radio wave,” [Online]. Available : http://en.wikipedia.org/wiki/Radio_waves
6. “Spectrum Analysis for Future LTE Deployments,” [Online]. Available: http://www.motorola.com/web/Business/Solutions/Industry%20Solutions/Service%20Providers/Wireless%20Operators/LTE/_Document/Static%20Files/LTE_Spectrum_Analysis_White_Paper_New.pdf
7. “Self-Optimizing Networks: The Benefits of SON in LTE,” [Online]. Available: http://www.4gamericas.org/index.cfm?fuseaction=pressreleasedisplay&pressreleaseid=3216
8. “Trial and error,” [Online]. Available: http://en.wikipedia.org/wiki/Trial_and_error
9. “Brute-force search,” [Online]. Available: https://www.princeton.edu/~achaney/tmve/wiki100k/docs/Brute-force_search.html
10. C. Y. Lee and H. G. Kang, “Cell planning with capacity expansion in mobile communications: a tabu search approach,” *IEEE Transactions on Vehicular Technology*, vol. 49, no. 5, pp. 1678-1691, September 2000.
11. P. Guo, X. Wang, and Y. Han, “The enhanced genetic algorithms for the optimization design,” In *Proc. 3rd International Conference on Biomedical Engineering and Informatics*, October 2010, vol. 7, pp. 2990-2994.
12. Dimitris Bertsimas and John Tsitsiklis, “Simulated Annealing,” Statistical Science, Vol. 8, No. 1, 10-15, 1993 [Online]. Available: http://stuff.mit.edu/~dbertsim/papers/Optimization/Simulated%20annealing.pdf
13. A. Awada, B. Wegmann, I. Viering, and A. Klein, “Optimizing radio network parameters of Long Term Evolution system using Taguchi’s method,” *IEEE*

Transactions on Vehicular Technology, vol. 60, no. 8, pp. 3825-3839 October 2011.

14. "Taguchi methods," [Online]. Available : http://en.wikipedia.org/wiki/Taguchi_methods
15. "Design of experiments via Taguchi methods," [Online]. Available : https://controls.engin.umich.edu/wiki/index.php/Design_of_experiments_via_taguchi_methods:_orthogonal_arrays
16. "Orthogonal array," [Online]. Available : http://en.wikipedia.org/wiki/Orthogonal_array
17. G. Taguchi, "Taguchi methods in LSI fabrication process," in *Proc. IEEE Int. Workshop Stat. Methodology*, pp. 1–6, Jun. 2001.
18. G. Y. Hwang, S. M. Hwang, H. J. Lee, J. H. Kim, K. S. Hong, and W. Y. Lee, "Application of Taguchi method to robust design of acoustic performance in IMT-2000 mobile phones," *IEEE Trans. Magn.*, vol. 41, no. 5, pp. 1900–1903, May 2005.
19. S. R. Karnik, A. B. Raju, and M. S. Raviprakasha, "Geneticalgorithm- based robust power system stabilizer design using Taguchi principle," in *Proc. 1st Int. Conf. Emerging Trends Eng. Technol*., pp. 887–892, Jul. 2008.
20. H. Ikeda, T. Hanamoto, T. Tsuji, and M. Tomizuka, "Design of vibration suppression controller for 3-inertia systems using Taguchi method," in *Proc. Int. Symp. Power Electron., Elect. Drives, Autom. Motion*, pp. 1045–1050, 2006.
21. K. L. Virga and R. J. Engelhardt, Jr., "Efficient statistical analysis of microwave circuit performance using design of experiments," in IEEE MTT-S *Int. Microw. Symp. Dig.*, vol. 1, pp. 123–126, Jun. 1993.
22. A. S. Hedayat, N. J. A. Sloane, and J. Stufken, *Orthogonal Arrays: Theory and Applications*. New York: Springer-Verlag, 1999.
23. A. Awada, B. Wegmann, I. Viering, and A. Klein, "A joint Optimization of Antenna Parameter in a Cellular Network Using Taguchi's Method," *IEEE Vehicular Technology Conference (VTC Spring)*, on page(s): 1-5, 73rd, 2011.
24. H. Xu, "An algorithm for constructing orthogonal and nearly-orthogonal arrays with mixed levels and small runs," *American Statistical Association and the American Society for Quality*, vol. 44, no. 4, Technometrics, November 2002.
25. 3GPP, "Physical layer aspects for evolved universal terrestrial radio access (UTRA)," *TR 25.814, Sophia-Antipolis, France, Tech. Rep*. 2006.
26. W.-C. Weng, F. Yang, and A. Elsherbeni, "Linear antenna array synthesis using

Taguchi's method: A novel optimization technique in electromagnetics," *IEEE Transactions on Antennas and Propagation*, vol. 55, no. 3, pp. 723–730, March 2007.

27. *Report ITU-R M.2135, Guidelines for evaluation of radio interface technologies for IMT-Advanced*, 2008. F. Gunnarsson, " Downtitled Base Station Antennas - A Simulation Model Proposal and Impact on HSPA and LTE Performance," *IEEE Vehicular Technology Conference (VTC Fall)*, 68th, on page(s): 1-5, September 2008
28. F. Gunnarsson, " Downtitled Base Station Antennas - A Simulation Model Proposal and Impact on HSPA and LTE Performance," *IEEE Vehicular Technology Conference (VTC Fall)*, 68th, on page(s): 1-5, September 2008
29. "Kathrein 742215 Data Sheet," [Online]. Available: http://www.kathrein-scala.com/catalog/742215V01.pdf.
30. P. Mogensen, W. Na, I. Kovacs, F. Frederiksen, A. Pokhariyal, K. Pedersen, T. Kolding, K. Hugl, and M. Kuusela, "LTE capacity compared to the Shannon bound," in *Proc. IEEE Veh. Technol. Conf.*, 2007, pp. 1234–1238.

Appendix

A. Using the Hybrid Approach in A Network of 11 eNodeBs

The proposed hybrid approach has been tested with many different initial settings of the configuration parameters and eNodeB locations. All the results are nearly the same as that of the single-NOA optimization, but the hybrid approach saved about 50% time in the optimization process. As the number of eNodeBs increases, the optimization time becomes longer. Fig. A-1 shows the 11-eNodeB network with 33 cells randomly located in a 2000 × 1000 m^2 area. All eNodeBs have the same parameters as that described in Section 5.4. There are 66 configuration parameters to be optimized.

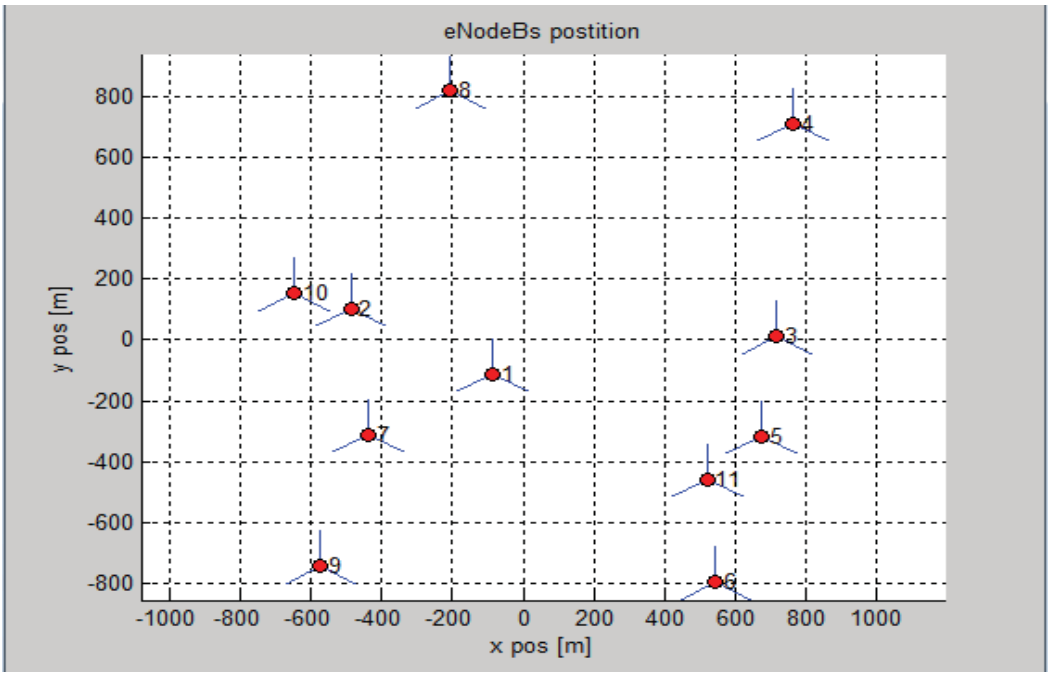

Figure A-1: LTE-A network with cells of different coverage areas and default azimuth orientations

Fig. A-2 shows the comparison of optimized 5%-tile CDFs F(x) of improved mixed-level NOA and identical-level NOA. It is clear that the improved mixed-level NOA gives better result than identical-level NOA. The iteration scheme is 6-3-13 which saves about 42% experiments in the optimization and achieves better result than the identical-level NOA method. Fig. A-3 presents the SINR map of the network before (left) and

after (right) the optimization using the hybrid approach. It is obvious that the optimized network has good SINR in most of the area, proving better coverage and throughput.

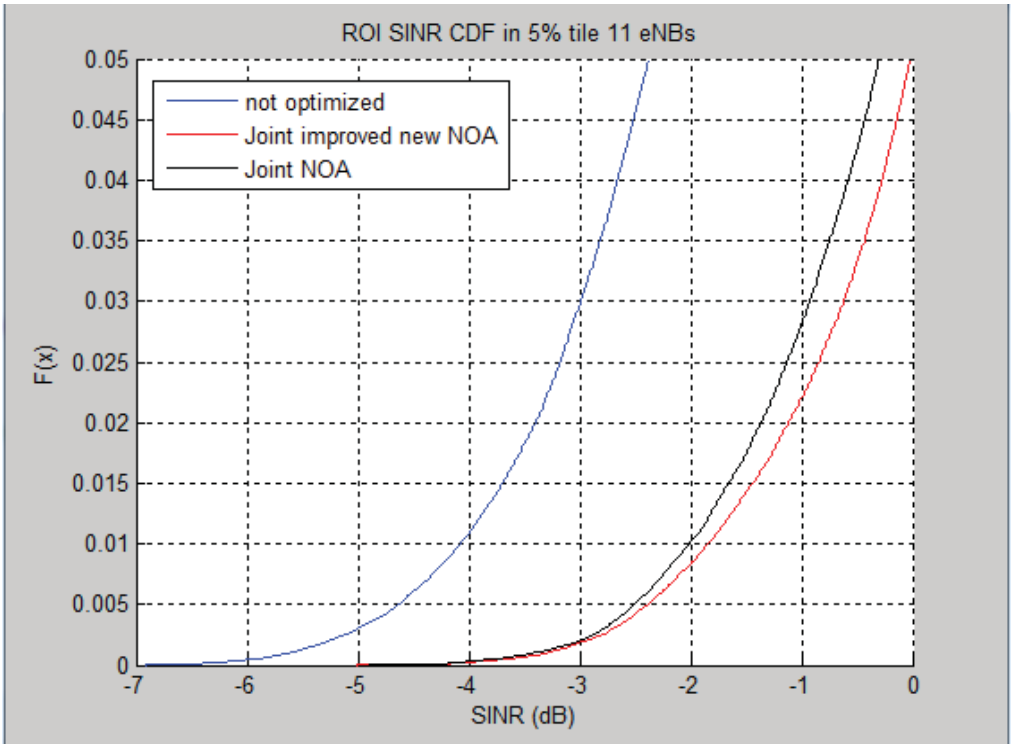

Figure A-2: Comparison of optimized 5%-tile CDFs of improved mixed-level NOA and identical-level NOA in a network of 11 eNodeBs

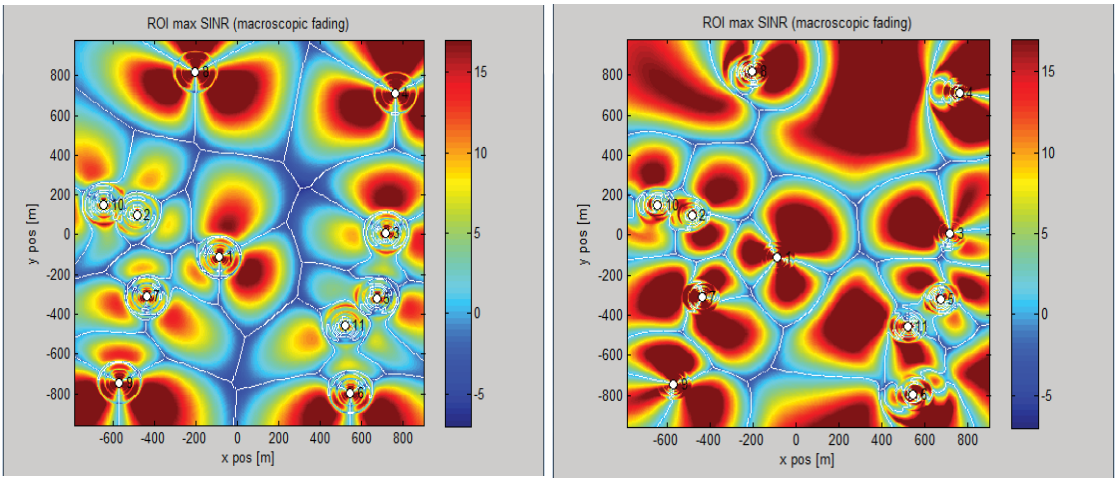

Figure A-3: Comparion of SINR map before (left) and after (right) optimization